

出國報告（出國類別：開會）

參加 2018 年地球物理探勘師學會年會  
並發表論文

服務機關：台灣中油股份有限公司

姓名職稱：邱維毅 地球物理探勘師

派赴國家/地區：美國

出國期間：107 年 10 月 12 日至 107 年 10 月 21 日

報告日期：107 年 10 月 24 日



## 摘要

SEG (Society of Exploration Geophysicists, 地球物理探勘師學會) 是一個極富盛名的非營利組織，除提供世界各國之地球物理學家、相關科系學生各種與地球物理相關之知識與課程外。更綜合各領域專家，出版許多專書，內容橫跨如何實際應用地球物理學於震測資料採集與處理、重力和電磁測勘、油藏地球物理、近表面地球物理、地球物理綜合解釋等方面。

本出國計畫藉由參與 2018 年 SEG 於美國加利福尼亞州安那翰市 (Anaheim, CA) 所舉辦之年度學術研討會，了解世界上最新的技術發展趨勢、技術應用成果、石油業聚焦競爭之探勘區域…等。此外，也藉此機會，報名參與會前之「Structural Geology in Seismic Interpretation」短期課程。該課程由具實際學界、業界經驗之 Shankar Mitra 教授所開設，自構造地質學概念出發，介紹拉張構造、岩鹽相關構造、擠壓構造、走向滑移構造與反轉構造之特性，並且講授如何將不同構造之特性應用於震測解釋上。經此課程，學習構造解釋工作所需注意的重點及需要思考的各種構造形貌可能性。

## 目錄

一、目的.....	1
二、過程.....	2
(一)出國行程.....	2
(二)訓練課程內容(10月13日~14日).....	2
(三)參與會議內容(10月15日~19日).....	4
三、具體成效.....	10
四、心得及建議.....	10
五、附錄 - 張貼海報內容.....	13
附錄 - 短期課程課堂筆記內容.....	17

# 一、目的

SEG (Society of Exploration Geophysicists, 地球物理探勘師學會) 成立於 1930 年, 是一個極富盛名的非營利組織, 除提供世界各國之地球物理學家、相關科系學生各種與地球物理相關之知識與課程外。更綜合各領域專家, 出版許多專書, 內容橫跨如何實際應用地球物理學於震測資料採集與處理、重力和電磁測勘、油藏地球物理、近表面地球物理、地球物理綜合解釋等方面。

SEG 每年定期舉辦的學術研討會, 更是全球與地球物理相關的公司、學者與學生均踴躍投稿及參加的會議。會議期間, 除各知名大學、大油公司、地球物理軟體及探勘服務提供公司皆會於會場設立講解攤位外, 會場更會舉辦多場專題演講向與會者分享最新的技術發展、應用成果, 可謂全球地球物理界的一大盛事。今年度(2018)之 SEG 年度學術研討會於美國加利福尼亞州之安那翰(Anaheim)市舉辦, 會議舉辦期間為 10 月 14 至 19 日。在會議開始前一日(即 10 月 13 日), 主辦單位提前開設一系列為期兩日的短期訓練課程。藉由參與 SEG 機會, 報名參與「Structural Geology in Seismic Interpretation」課程。該課程由構造地質學概念出發, 介紹拉張構造、岩鹽相關構造、擠壓構造、走向滑移構造與反轉構造之特性, 並且講授如何將不同構造之特性應用於震測解釋上。

參與年度 SEG 年度學術研討會能除接觸並蒐集地球物理探勘技術最新發展趨勢, 並期望可藉由課程, 學習構造解釋工作所需注意的重點及需要思考的各種構造形貌可能性。

此外, 本所傅式齊副所長投稿並獲 SEG 會議接受之論文「Plio-Pleistocene biogenic gas systems and their unconventional resource potential in the Chianan Plain, southwest Taiwan」, 因傅副所長公務繁忙之故, 故由本計畫申請人代為於 107 年 10 月 17 日以張貼海報形式發表。

## 二、過程

### (一)出國行程

出國期間:107 年 10 月 12 日至 21 日，共 10 天。

出國行程:

- 1、10 月 12 日(星期五)，自桃園機場搭乘長榮航空 BR6 班機於 10:10 啟程。
- 2、10 月 13 日~14 日，參加「Structural Geology in Seismic Interpretation」訓練課程，課程地點為 Anaheim Convention Center。
- 3、10 月 15 日~19 日，參與 2018 年度 SEG 年度學術研討會
- 4、10 月 20 日~21 日，搭乘長榮航空 BR5 班機返程。

### (二)訓練課程內容(10 月 13 日~14 日)

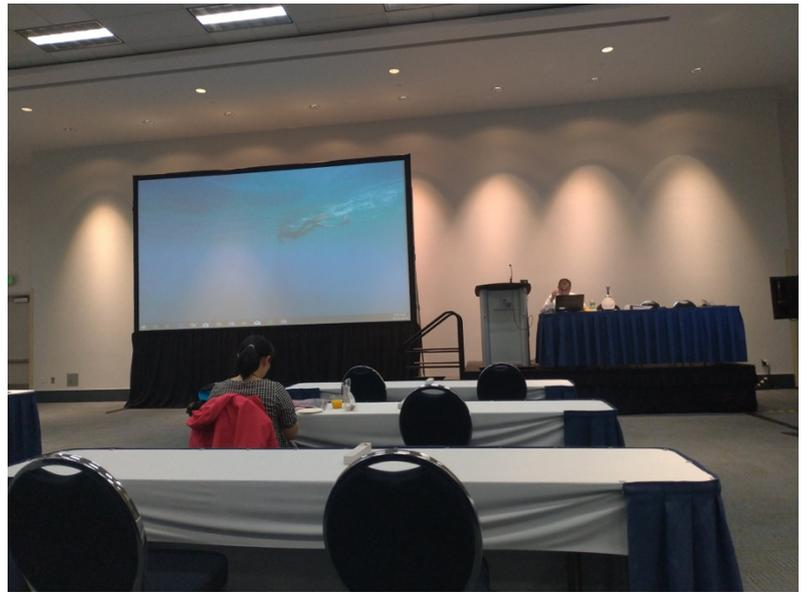
「Structural Geology in Seismic Interpretation」課程講師為 Shankar Mitra。Shankar 教授任教於奧克拉赫瑪大學 Mewbourne 地球與能源學院 (Mewbourne College of Earth and Energy)內的地質與地球物理學院(School of Geology and Geophysics)。Shankar 教授將構造地質學應用於石油勘探和生產工作，至今已有超過 35 年的從業與學術經驗。其於 1977 年獲得約翰霍普金斯大學結構地質學博士學位，曾於 ARCO 公司之研究和勘探部門任職達 19 年，先後擔任高級和首席研究地質學家、構造地質學主管，地質研究經理、歐洲地區探勘總監和高級勘探研究顧問，研究區域遍及全球。

其專長為構造地質方法的發展及其在勘探和生產問題中的應用，並曾兩次獲得 AAPG 的華萊士普拉特最佳論文獎和 Cam Sproule 最佳論文獎。因此，Shankar 教授可謂是全球構造地質學界之翹楚。

該課程討論了拉張構造、岩鹽相關構造、擠壓構造、走向滑移構造與反轉構造之構造特性、構造形貌、如何應用於解釋結構及可能的構造多解性與不確定性，並藉由展示世界各地實際產出油氣資源構造的震測影像實例，據以輔助說明常見的構造樣式及其震測影像特徵。除此之外，亦討論各構造形貌可能產生的震測影像缺陷與如何利用構造平衡、構造回復方法驗證震測解釋。

由於課程內容篇幅較多，因此課堂筆記內容以附加檔案方式置於本出國報告之附錄部分。在此僅列出以下幾點 Shankar 教授一再強調應用構造地質概念於震測資料解釋時須注意的基本守則與要點：

1. 在震測資料品質不佳之複雜構造區域，震測解釋無法得到可靠的成果。
2. 構造概念具有引導震測解釋（特別是成像品質不佳的震測資料、位置），可應用構造繪圖原理與概念進行成像不良區域的解釋。
3. 在進行震測資料解釋前，須先了解震測資料處理速度是否合理、是否符合地質概念。特別是進行 PSDM 震測資料解釋時，需了解 PSDM 進行震測資料處理時所導入的地質概念與速度模型是否符合研究區域之狀況。不符現地狀況的 PSDM 震測資料處理構造概念與速度模型，會造成 PSDM 最終資料處理結果與實際地下地質狀況大相逕庭。
4. 在斷層斷距大或是有局部橫向速度變化劇烈的區域，會因速度差異造成下推 (pushdown) 或上拉 (pull up) 現象，產生假的構造高區或低區，影響構造判斷。
5. 進行震測解釋時，須隨時注意構造的合理性、是否平衡。
6. 相同的構造區域 (tectonic regime) 可能會有類似構造重複出現的狀況，解釋時可應用已證實之同一區域鄰近構造的樣貌建立解釋前的構造概念。
7. 相同的應力狀態，可能會有不同的構造型貌發育（如：張力環境下，可能出現平面斷層或鉞形斷層，因此，解釋前須先了解目標區的構造概念。



「Structural Geology in Seismic Interpretation」課程教室

### (三)參與會議內容(10月15日~19日)

今年度(2018)SEG共審閱了超過1800篇來自全球各單位的研究成果，其中有1080篇被接受。這些論文分別於26個不同主題的會議廳中發表，共計151個場次。以下分別為個主題之研究內容：

1. Acquisition and Survey Design	2. Passive Seismic
3. Anisotropy	4. Reservoir Characterization
5. AVO and Seismic Inversion	6. Rock Physics
7. Borehole Geophysics	8. Special Global Session
9. EM Exploration and Reservoir Surveillance	10. Seismic Modeling
11. Full Waveform Inversion	12. Seismic Processing: Emerging Technologies
13. Gravity and Magnetics	14. Seismic Processing: Migration
15. Interpretation	16. Seismic Processing: Multiples, Noise, and Regularization
17. Mining	18. Special Session
19. Machine Learning and Data Analytics for E&P	20. Seismic Theory
21. Multi-Physics Data Integration	22. Seismic Velocity Estimation

23. Multicomponent Seismic	24. Time Lapse
25. Near Surface	26. Vertical Seismic Profile

本次與會主要著重於聆聽構造解釋、岩石地球物理與自動追蹤解釋之議題。其中，與震測解釋相關之斷層自動追蹤研究，多集中於卷積神經網路(convolution neural network, CNN)之研究。卷積神經網路是近幾年來研究深度學習探討的重點，以往多應用於電腦影像視覺研究上，亦即偏重於資工學門之研究。但由於震測料亦可視為一種影像類型，因此，如何應用與改進 CNN 演算法，成為研究自動化震測解釋的熱門研究主題。綜觀於會場所發表之 CNN 應用於自動斷層識別研究成果可發現，研究目標幾乎都以拉張構造為主，此現象其實非常合理，因為拉張構造，特別是以平面斷層為主的海域構造，震測影像一般較為清晰且品質佳，可作為研究之切入目標。由於 CNN 方法是基於影像識別的方法，因此會場有些研究成果著重於討論傳統強化斷層影像之方法；或是藉由學習人工識別規律輔助 CNN 計算；或利用濾波、方向門檻值設定等手段加強 CNN 識別合理性…等等之研究。但是，亦有研究完全迥然於前述研究手段相反，其基於人工設定模擬隨機分佈之水平變化反射係數，結合對稱與不對稱構造模擬、垂向影像剪切、隨機斷層模擬、子波摺積與隨機雜訊分佈…等手段產生具斷層之人造震測影像，分別建立可供機器學習之不同走向與傾角之斷層影像資料庫（~900,000 種正斷層學習影像），再根據該資料庫，應用於辨識實際震測資料內之斷層分佈。以上觀看現場以各種不同角度出發所得到的不同計算、研究方法之研究成果，著實令人大開眼界，充滿驚喜。

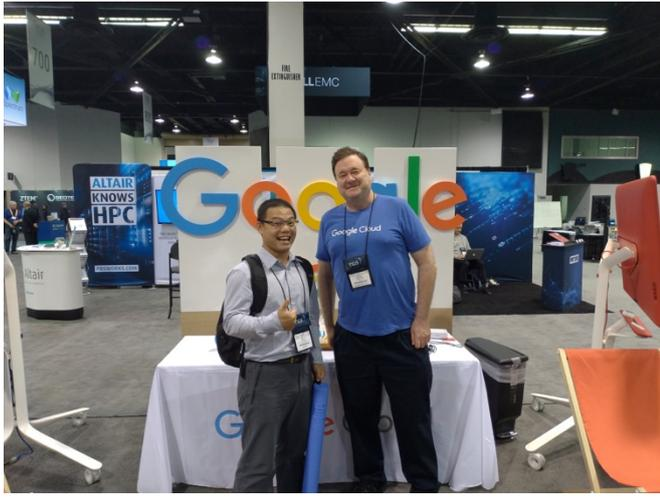
但是，在自動影像識別的研究上，本人實際至展覽會場詢問 Schlumberger 技術人員有關該公司未來是否會推出 CNN 計算的套件，其回答令人更加驚訝。該公司並沒有推出單機運算 CNN 套件的規劃，而是會結合各種構造型態與震測資料於該公司正積極發展的雲端系統 DELFI 中，以大數據分析的方式，發展自動化斷層與構造解釋功能，並且應用於辨識震測影像中之油氣分佈。該系統預計將整合探勘、模擬、設計、開發、監控等資料於雲端系統，因此可更有效率的運用計算能力及資源於複雜構造的油氣探勘開發。

雲端應用層面上，會場各大服務公司（Schlumberger、Emerson、DownUnder GeoSolutions、iKon）都推出雲端運算與儲存的服務規劃。也因為如此，Google、hp、Dell、Western Digital 等公司都於現場設有攤位，搶攻石油業的商機。就此角度看

來，雲段數據庫與運算勢必為未來石油探勘業發展的趨勢，如何快速的整合資料、多領域資料結合解釋、基於大數據進行構造、儲集層識別並作出決策，將是推動與加速探勘步調的重要推手。

在陸域震測資料採集技術方面，無論是參展設備商或是服務商，都集中火力在推展無線化的震測資料採集設備，有別於以往的陸域震測需大規模展佈帶纜線檢波器的施測方式，為了提高工作效率與深入困難地區的資料採集速率，無線檢波器將是未來陸域震測的主流。其中較特別的是 Total(GeoExPro)公司所展出的空投式檢波器，其主要應用於叢林、雨林等踏無人跡或難以以傳統佈線方法探勘的區域。可利用無人機載運的方式，精確的空投至規劃點位，並將所接收到的訊號以無線傳輸的方式傳遞至基地接收站。利用這樣的方式，可大幅減少環境的破壞、降低調查人員的傷亡風險、探勘時間與施測開銷，並可於施測現場的 Fast-Stack 資料資料品質控制中，即時以無人機投送檢波器密度於資料品質較不佳的區域，提升區域震測資料品質。

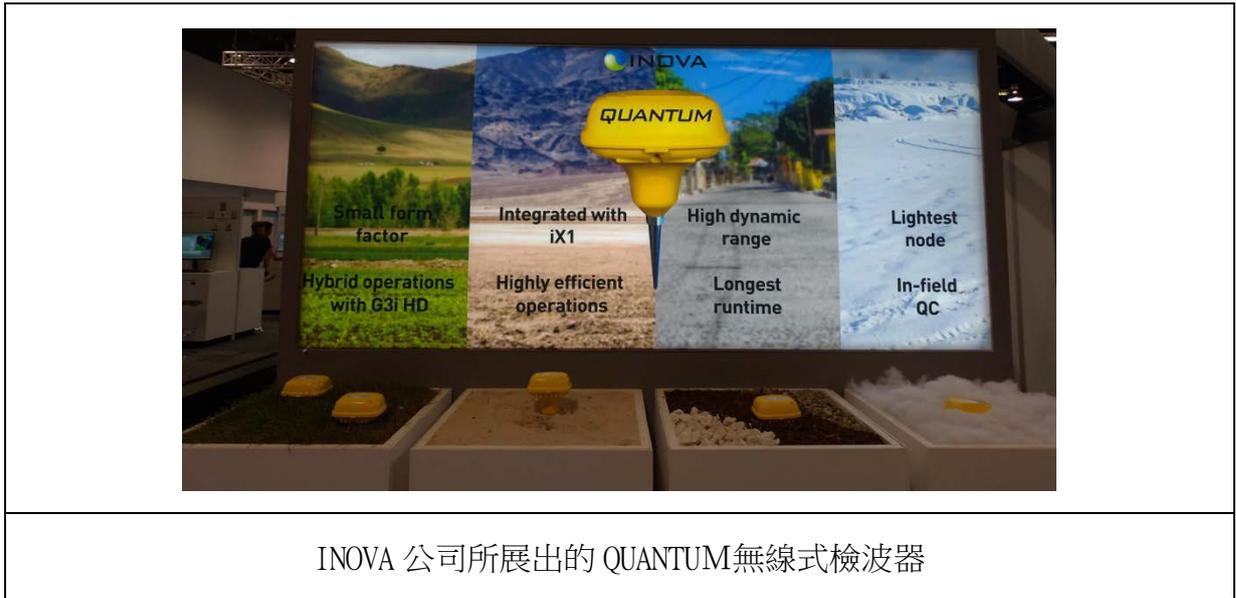
海域震測資料採集與處理方面，除了過往所強調的寬頻資料與寬方位角(Wide Azimuth, WAZ)震測，會場無論是震測公司或是服務公司都更為強調更為低頻資料的採集與全方位角(Full Azimuth, FAZ)資料的採集與應用。在施測方面利用海底地震儀節點化分佈、結合類似 PGS 公司所推出之 GeoStreamer 與矩陣化震源，可減少海水面複反射與雜訊。並藉由 Q tomography、Anisotropic estimation、Least-Squares Reverse Time Migration (LSRTM)…等手段，達到提高速度模型準確性、增強震測影像與低頻訊號、消除雜訊等目的。另外，現場更分別有不同公司與研究單位展示或討論(Total、PGS、GPUSA、日本東京大學)海域震盪震源(Marine Vibrator Sources)，此種震源產生方式類似陸域震盪震源車，可人工控制震源震盪時間與頻譜分佈(頻率可低至 2-6Hz，主頻可調控 5~100+ Hz)，不需壓縮空氣且對生物的衝擊性較傳統空氣槍方式更小(無論是 sound pressure level ,SPL 與 sound exposure level, SEL)。此種施測方或將成為未來海域資料採集的主流。



Google 公司及 Dug 公司所展出之攤位。無論是石油服務商或是雲端技術提供公司，都在強調利用具強大運算能力及儲存能力的雲端設備，提高探勘開發資料整合效率與計算能力的雲端解決方案。未來使用者端將由目前的單機工作站設置，走向所有計算與儲存接雲端化的時代，單機功能僅是工具介面的展示。



Total(GeoExPro)公司所展出的空投式檢波器



INOVA 公司所展出的 QUANTUM 無線式檢波器

Retractable for transit/storage

All underwater components housed in a sealed stainless steel enclosure

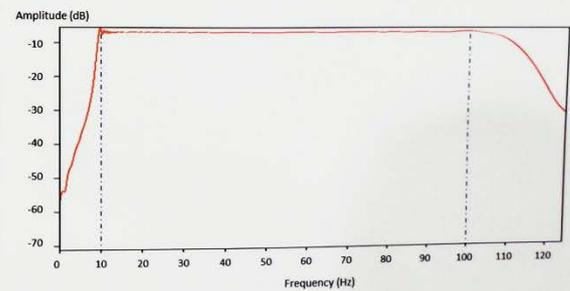
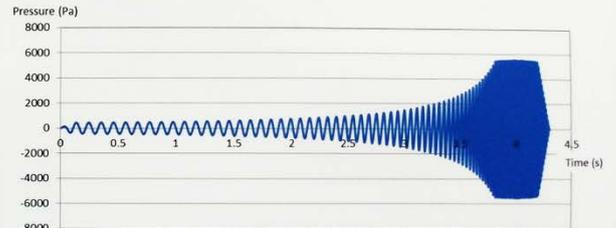
MV-32 SPECIFICATIONS*		
Parameter	Units	Value
Frequency Range	Hz	0 -100
Sound Pressure Level (at 100 Hz)	dB re 1µPa/Hz	>200
Weight (Source Module)	lbs.	160 (approximate)
Diameter (Source Module)	in.	36
Width (Source Module)	in.	12
Source Drive Motor Rating	horsepower	6.3
Efficiency (@ Full Load)	%	>85%
System Power Requirement	volts/Hz	480V, 3Phase/50-60
Maximum Operating Depth	feet	30
Minimum Operating Depth	feet	3
Source Module Max. Duty Cycle (in water)	%	100
Operating Temperature Range (Wet End)	Degrees F	0 to 100
Operating Temperature Range (Surface Electronics)	Degrees F	32 to 130

\*Subject to change w/o notice

GPUSA 所設計的 MV -32 Marine Vibrator Sources 運作示意圖及其產品參數

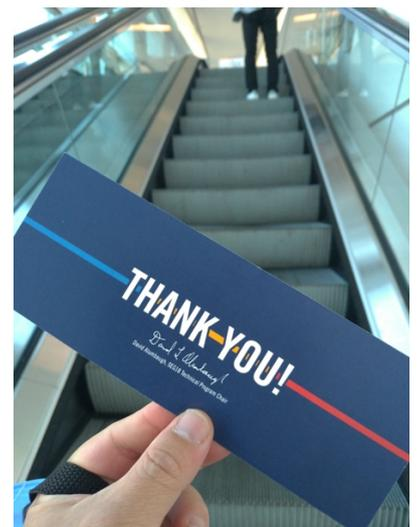
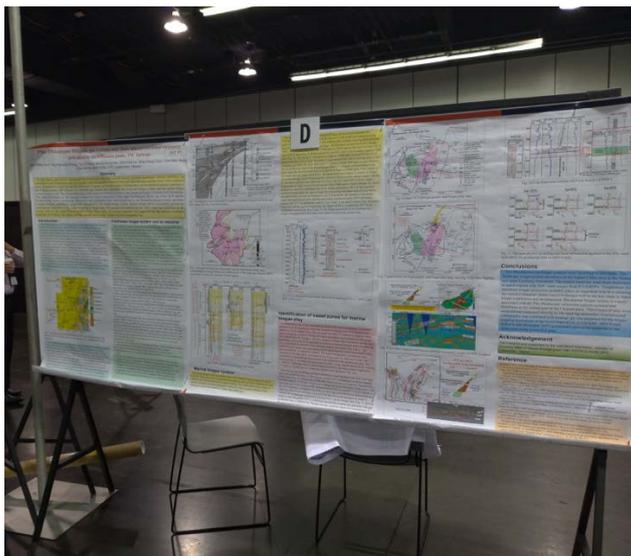
### Fig.3 Downsized Marine Seismic Vibrator (MSV)

MSV is designed to employ a hydraulic servo system for the controllability on the signal generation both in the phase and in the amplitude for a frequency band ranging from 3 to 300 Hz. In the survey in Fig.2, we designed a source signature of upward sweep of a 4 second long of a flat spectrum band from 10 to 100 Hz.



Waveform generated by Downsized MSV

日本東京大學進行研發與測試中的 Marine Seismic Vibrator(MSV)



本次會議代替探探研究所傅式齊副所長於現場張貼研究成果海報並宣讀。上圖即為張貼海報現場與報告完後獲得的小禮物交換卷。

### 三、具體成效

藉由參加本次 SEG 年會，除實際了解探勘最新資訊外，更攜回各油公司與服務公司之最新技術簡介，供本單位參考。有關之陸、海域資料採集技術、探勘技術發展熱點與國際油氣探勘趨勢如本報告內容與建議所示。

另外，現已將會前短期課程講義及課堂筆記(如本報告第五部分)置於本單位及探採事業部共享資料夾內，提供予有興趣之同仁參酌。再者，擬將短期課程內所提及之構造地質學解釋概念、震測解釋注意事項與速度資料體品質確認等流程，應用於今年度「高屏外海油氣潛能評估計畫」及 108 年度「台灣中油-哈斯基深水合作礦區油氣潛能評估」石油基金研究計畫之震測資料解釋工作，期可縮小震測解釋之不確定性與提高可信度。

### 四、心得及建議

1. 現場得知 Schlumberger 公司所研發之 Petrel 2108 功能已包含重合前(pre-stack)資料基本整理與編輯功能。由於本公司剛與該公司簽訂五年期之租賃合約，但在 Petrel 2018 版本釋出時，本公司探勘單位已擬訂之未來兩年軟體購置計畫，其中即包含購買重合前資料編輯軟體。建議可再進行現有軟體功能盤點與擬購軟體功能比較，以免重複購買具相近功能之軟體，以期有效運用軟體採購經費。
2. 無論是石油服務商(Emerson、DownUnder GeoSolutions、iKon)或是雲端技術提供公司(Google、hp、Dell...), 都在強調利用具強大運算能力及儲存能力的雲端設備，提高探勘開發資料整合效率與計算能力的雲端解決方案。未來使用者端將由目前的單機工作站設置，走向所有計算與儲存皆雲端化的時代，單機功能僅是工具介面的展示。與其把經費投入在眾多運算與儲存能力有所侷限的單機計算功能提升上，或許可考慮現有商業界所提供的整合性平台獲解決方案(如 google、Dell EMC...), 以雲端運算儲存的方式，建立本公司的探勘、設計、開發與監控系統。

3. 展覽會場眾多參展的單位中，與其他攤位有所不同的是科威特石油公司的展示，該公司展示主要的目的之一即為介紹該國未來的投資機會。目前該國正尋求外國公司投資其國內的探勘與開發，包含了重油開發、海域油氣田探勘、油田增產與非伴生氣的開發…等機會。由於科威特生產原油已久，有許多油公司及服務公司參與於該國國內市場，因此算是油氣探勘開發相對成熟的國家。此外，主辦單位特別開設了一系列的主體演講，旨在展示、討論與展望墨西哥所屬墨西哥灣海域油氣田開發的現況與未來發展，雖然該國開放石油探勘年代較晚，但由於該國海域與北墨西哥灣（近美國側）之地質背景相似，基於美國所屬墨西哥灣的成功探勘開發經驗，所以南墨西哥灣（近墨西哥）的油氣田礦區競標為美州大陸上除巴西外海礦區外最為活躍的地區之一。因本公司探勘管理階層一再強調提升台灣自主能源的重要性，而以上兩區域皆為有良好技術基礎、已證實石油系統與遠景的油氣產區，建議本公司可積極接洽這些地區的油氣礦區標售與合作機會，讓中油公司探勘部門可以在探勘事業上更為穩健及有競爭力。
  
4. 經由參與「Structural Geology in Seismic Interpretation」課程，才驚覺震測解釋前Q C 速度資料的重要性。唯有先了解震測資料處理的速度構造是否合理，才可基於對地區的認識進行正確的資料解釋，否則可能會將因速度變化所產生的 Pullup 或 Pushdown 當成是真實現象解釋，造成好景區識別的誤判。也唯有瞭解不同構造於震測成像上的侷限和相似性，才可跳脫反射的限制，進行符合地質與構造概念的解讀。
  
5. 中油公司雖然是國內最大的能源公司，但就探勘領域而言，相對於國外主要油公司或服務公司，可說是小巫見大巫。本公司全體探勘事業人員一千多人，應屏棄國內最大油公司之自傲以及面對大國之自卑，戮力發展具有足夠技術與評估能力的工作小組及團隊，積極突破、接洽並參與國外探勘或生產礦區之合作機會，藉由中長期借調人員的機會培養人員的技術能力。或是借鏡國外其他轉型成功之油公司，聘雇

專業顧問（或公司）之礦區管理與營運長才，進行轉型。沒有實際油氣收入，就不可能維持探勘事業之運作，更何況是技術發展。既然發現了危機就應尋找轉機，而非抱持國營事業鐵飯碗的心態坐以待斃。

## 五、附錄 – 張貼海報內容

# Plio-Pleistocene biogenic gas systems and their unconventional resource potential in the Chianan plain, SW Taiwan

INT P3

Shi-Chie Fuh\*, Kuo-Hsiung Chang, Tzy-Yi Chang, Shiang-Horng Hsu, Shih-Chia Lin, Bing-Cheng Chen, Chih-Wen Wang, Chia-Yen Ku, Wei-Yi Chiu, (CPC Corporation, Taiwan)

## Summary

In this study, previously interpreted Plio-Pleistocene submarine canyon system, inverted impedance, seismic attributes, log correlation and evaluation, mud log anomaly, depositional facies observed from core and outcrops, and the source rock evaluation were integrated to build up the Plio-Pleistocene biogenic gas systems and to evaluate their unconventional resource potential in the Chianan plain, SW Taiwan. Two biogenic gas systems were identified, the freshwater biogas system and the marine biogas system respectively. The former distributes to the southwest and east of Chiali in the Tainan and upper Liushung (LS) formations. The latter distributes to the east and northeast of Chiali in the lower LS/the upper Eurchungchi (ECS), the lower ECS and the Kanhsiaoliao (KSL) formations. Three brine gas exploration plays were recognized in the freshwater biogas system and three residual biogas exploration plays were recognized in the marine biogas system. Recent drilled HSY-8 accidentally proved the residual gas potential of the lower Eurchungchi biogas play. The prospect associated with the HSS-1 well was identified as the sweet zone of the upper Eurchungchi/Liushung biogas play. Its resource potential was supported by the seismic sweetness attribute of 10 Km<sup>2</sup>, the strong mud log anomaly and possible channel related stratigraphic trap.

## Introduction

Plio-Pleistocene conventional biogenic gas potential in the southwestern onshore Taiwan has been previously studied (Fuh et al., 2003, 2009). Plio-Pleistocene submarine canyons developed in different geological time have been mapped. It was concluded that the major source rock associated with biogas generation were mainly deposited in the submarine canyons. It was not until 2012, after the communication between Shi-Chie Fuh and Paul Mendell, the unconventional biogas potential was paid attention by Exploration & Development Research Institute, CPC Corporation Taiwan. Hsu's study (1984) brought Paul's interest in looking after the Plio-Pleistocene brine/residual biogas exploration opportunity in the Chianan plain, SW Taiwan (Mendell, 2012). Siltstone with smaller pore throat has better chance to trap residual gas or brine gas (dissolved-in-water gas) along the gas migration path which requires no structural or stratigraphic traps as the conventional gas trapping mechanism does (Berkenpas, 1991). Existence of strong gas shows in shallow water wells in the Chianan plain has been known for a long time which invoked the attention of CPC Corporation, Taiwan to explore the brine gas potential from 1980 to 1982. During this period, 6 brine gas wells have been drilled in the Annan-Chiku area (Fig. 1).

## Freshwater biogas system and its resource

Three sequences and the corresponding depositional facies were analyzed based on whole cores from 14 groundwater observation wells (Huang, 2001).

The Tainan formation, equivalent to sequence 1 deposit, mainly deposited in a incise valley formed during the last glacial period. The depositional facies includes flooding plain, the estuarine mud and sand, tidal channel, meandering channel sand, the landward marsh and inner offshore deposits (Fig. 2).

The depositional facies of upper Liushung formation, equivalent to sequence 2 deposits, is similar to those of sequence 1. Relative low salinity content revealed by observing the resistivity and gamma log characters is consistent with the freshwater facies revealed from core. We concluded that low salinity water collected during production test reflects its original estuarine to territorial freshwater depositional environments rather than invasion of meteoric water. The stratigraphic architecture in the Annan-Chiku area is very similar to that of shallow biogenic gas reservoirs in the Hangzhou Bay area (Li and Lin, 2010).

Source rock evaluation has been conducted in this study for 31 core samples from marsh and lagoon facies. Four out of fourteen samples, the TOC values are greater than 0.5% (Fig. 2). The averaged TOC value for samples extracted from lagoon facies is 0.4±0.19%. That extracted from marsh facies is 0.35±0.18%. Ten depositional facies maps corresponding to 40000, 25000, 19000-17000, 17000-15000, 15000-13000, 13000-11000, 11000-9000, 9000-7000, 7000-5000, and 5000-3000 years ago respective (Huang, 2001), were used to analyze the freshwater biogas play types and their elements, respectively.

Source rocks for play type A are muds/shales deposited in marsh or lagoon around 40,000 years ago. The reservoir rocks are sands deposited in the flooding plain and meandering channel around 25,000 years ago. The seal rocks are muds/shale deposited in lagoon or marsh around 19,000-13,000 years ago.

For play type B, the source rocks are muds/shales deposited in marsh or lagoon around 40,000-11,000 years ago (Fig. 3). The reservoir rocks are sands deposited in the flooding plain and meandering channel around 17,000-11,000 years ago. The seal rocks are muds/shales deposited in marsh or lagoon around 9,000-3,000 years ago.

For play type C, the source rocks are muds/shales deposited in marsh or lagoon around 17,000-13,000 years ago. The reservoir rocks are sands deposited in the flooding plain and meandering channel around 13,000-3,000 years ago. The seal rocks are muds/shales deposited in marsh or lagoon around 3,000-1,000 years ago. The screen pipe locations, the submergible pump depths, and the casing intervals were marked on the Gr and resistivity log display panel for each well (Fig. 4). The different horse power applied during the production test and the test results were also examined. The failures of the production test for most of the wells were concluded as follows:

- 1) Very fine to fine sand grain of the freshwater biogas system associated with the paleo-Tsengwenchi River led to severe sand production problem.
- 2) Pumping period was too short to reflect the actual gas performance.
- 3) Matching between the installed screen depth and the reservoir sand depth was poor.
- 4) Instead of setting screen completion, the casing completion was set in the Tainan and upper LS formations. Therefore the dissolved-in-water gas was blocked and not able to come out from the reservoir of play type C. Temperature for maximum biogas generation is normally around 38°C-60°C (Kallmeyer and Wagner, 2014; Schneider et al., 2016). This optimized temperature in the Annan-Chiku area is unknown and may play a very important role in evaluating the brine gas resource potential in the area.

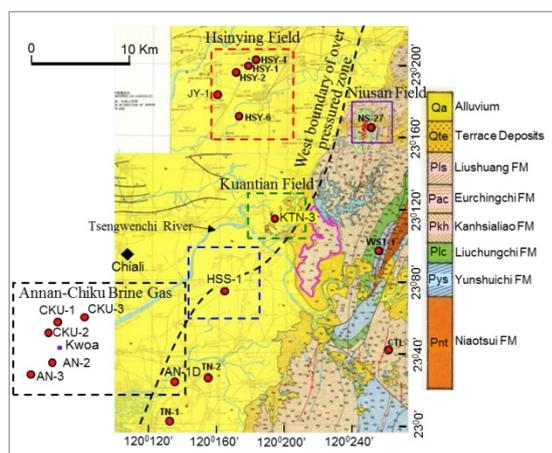


Fig. 1 The study area includes the Hsinying (HSY) gas field in the north, the Kuantian (KTN) gas field in the east and the brine gas exploration area in the southwest.

The well depth ranges from 300 to 997 meters. Production test has been applied to these wells and other 8 private water wells. Only Kwoa's private water well performed the best with gas rate of 5788 M<sup>3</sup>/D. Those of the rest wells are much poorer. Hsu (1984) concluded that the gas dissolved in the connate water has been destroyed by invasion of meteoric water. By reviewing the previous brine gas exploration works done from the points of engineering, geological, geochemical and geophysical views, we like to re-evaluate the brine gas potential in the area. By integrating the understanding of the unconventional biogas resource evaluation gained through this review work and the previously built stratigraphic frames in the Chianan plain (Fuh et al., 2003, 2009), we intended in this study to build up the Plio-Pleistocene biogenic gas system and to evaluate its unconventional resource potential in the whole Chianan plain.

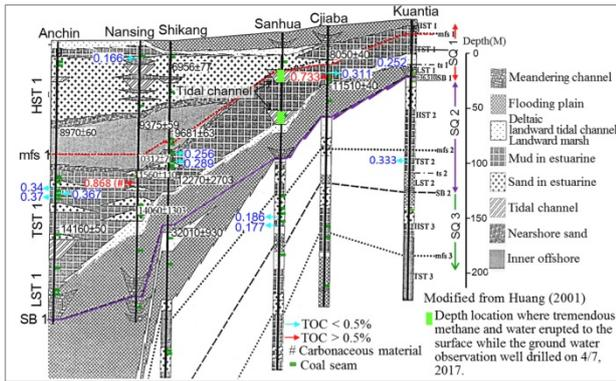


Fig. 2 Stratigraphic cross section shows sequence boundary, depositional facies and TOC values. See Fig. 3 for line location.

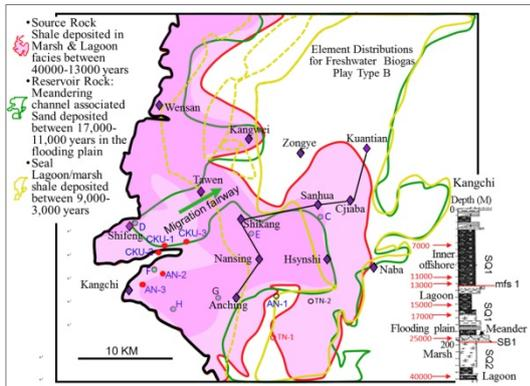


Fig. 3 Elements for freshwater biogas play type B. Depositional facies maps corresponding to the period between 40000 years to 3000 years ago (Huang, 2001), were used to analyze the elements for play type B.

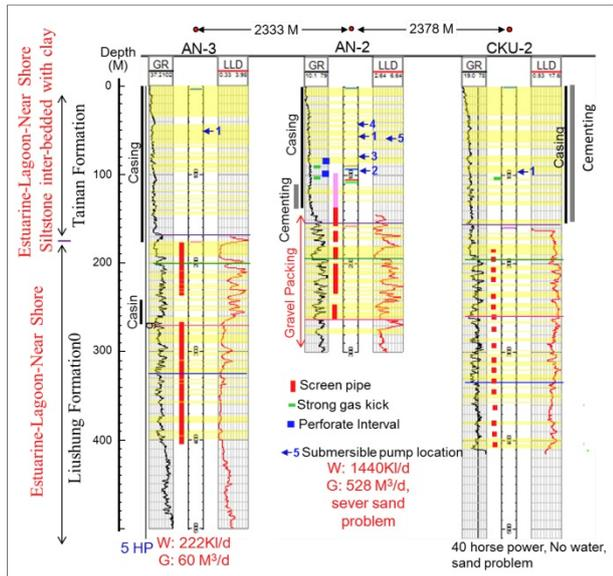


Fig. 4 Well completion and brine gas test results.

### Marine biogas system

The marine biogas system presented in the older formation such as lower LS, ECS and KSL. Three plays were recognized from south to north and their distributions were related to the Taiwan Mountain building evolution. The source rock of this system is mainly associated with Plio-Pleistocene submarine canyon system. Salinity of the formation water in the reservoir is higher than 30000 ppm.

The mud log anomaly detected during drilling is an important indicator for evaluation of the residual gas trapped in the reservoir with small pore throat or in the shale where biogas been generated. We collected all available mud log data and used in generating the marine biogas play maps. Background content level of C1 in the HSS-1 well jumped from less than 5000 ppm to 15000 ppm at the interval from LS\_A base to ECS base (Fig. 5). Right passed the top KSL, the C1 level reduce back to 5000 ppm (Fig. 5). The strong C1 anomalies as high as 50000 ppm occurred in the LS\_A sand and in the ECS\_b sand. The latter is equivalent to the 2nd producing zone of the Kuantian gas field. The silty sand with C1 content around 3000 ppm is equivalent to the 1st producing zone of the Kuantian gas field. C1 contents corresponding to the shale intervals between sand reservoirs can be as high as 25000 ppm. TOC values of the shale intervals range 0.4-0.66 %. We interpreted these high C1 content as biogas generated through micro bioprocess at a shallower buried depth. deeper depth. Similar C1 anomaly patterns were observed for CLI-1, the JY-1 and HSY-4 (H-4). Since temperature at shale interval buried greater than 1000 meters might mitigate the micro bioprocess, therefore eliminates the active biogas generation. We call the methane contained in the shale the paleo-biogas. By integrating the paleo-depositional facies revealed in the outcrops at Pachangchi and Tsengweichi, the salinity of formation water, the mud log anomaly, and the previously interpreted early ECS submarine canyon and ECS\_1a submarine canyon (Fig. 6 and 7), the paleo-coastal line, the paleo-hinge line and the marine biogas play for Upper ECS/LS\_A and lower ECS were interpreted respectively (Fig. 6 and 7). The biogas generated in the Kanhsialiao bios was preserved in the shale even further buried to the present day.

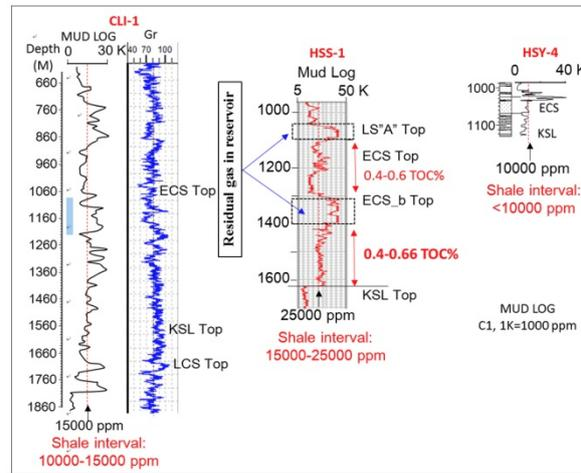


Fig. 5 C1 concentration anomalies observed on mud log of CLI-1, HSS-1 and HSY-4 (H-4) wells.

### Identification of sweet zones for marine biogas play

To further prove the biogas potential revealed by the mud log anomaly, sweetness attribute analysis (amplitude reflection strength divided by root of frequency) was applied to 16 2D seismic lines. The two intervals with C1 contents as high as 50000 ppm corresponds to the two strong sweetness anomalies on sweetness profile of line 81LTHSDB (Fig. 8). Up-dip to the NE, strong sweetness also was shown for the two producing zones at the KTN gas field. Extracted sweetness horizon attribute along the LS\_A time horizon showed a liner anomaly feature of 10 km<sup>2</sup> (Fig. 8 & 6). The reservoir in the sweet zone was interpreted as shelf channel system associated with a down-stream LS\_A submarine canyon. The same stratigraphic architecture was observed in the older ECS\_1a formation (see Fig 6. and 9). This sweet zone was interpreted as conventional stratigraphic trap combined with residual gas play. The high mud log C1 anomaly was penetrated by HSS-1 at the depth interval from 1040 M to 1080 M. DST failed due to mud invasion caused by the heavy mud weight up to 1.22 gm/c.c. Neither gas nor water was tested in the operation (Fig. 10)

The rock physics modeling and fluid substitution were applied to the silty sand right above the producing zone in HSY-4 well. At least 30% residual gas could be trapped in this sand (Fig. 11). Resistivity of this silty sand is as low as 2 ohm-m. Therefore it has been ignored in the past, despite this residual gas sand distributes further down dip across the gas/water contact in the non-production HSY-2 and HSY-7 wells. Based on the well impedance histograms for different lithology, a threshold was determined and applied to the horizon attribute extracted from the inverted impedance in order to identify the residual gas sweet zone of Lower ECS marine biogas play (Fig. 7). HSY-8 drilled in late December 2017, accidentally proved this residual gas potential with gas production rate of 4900 M<sup>3</sup>/D. The gas test rate would be improved tremendously if the sand control problem can be overcome.

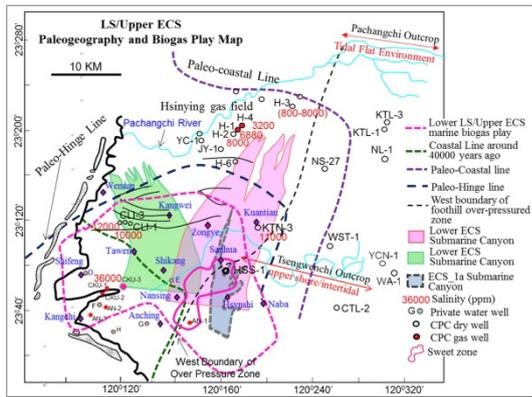


Fig. 6 Upper ECS paleogeography and biogas play map.

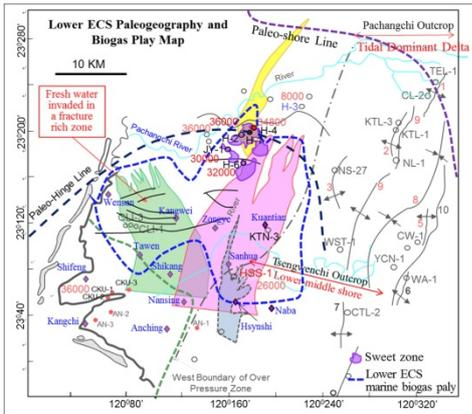


Fig. 7 paleo Lower ECS geography and biogas play map. See Fig. 6 for other legends.

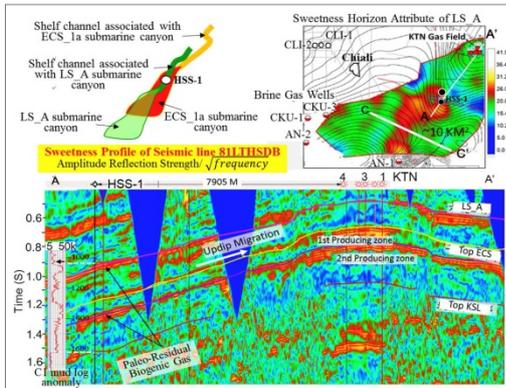


Fig. 8 Sweetness analysis and horizon attribute extraction results for HSS prospect.

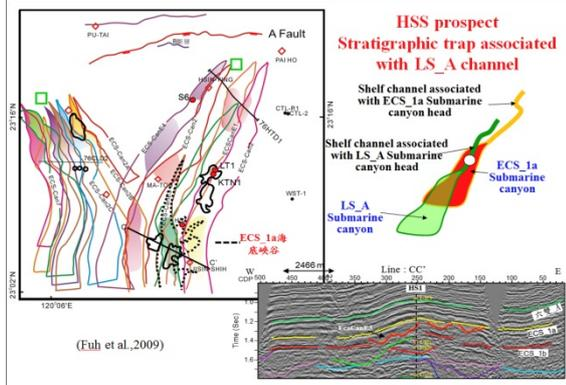


Fig. 9 Seismic interpretation of ECS\_1a submarine canyon.

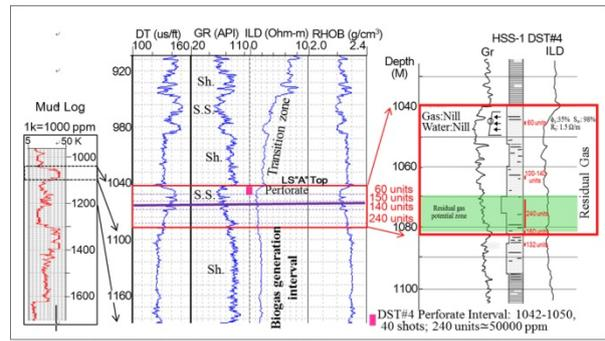


Fig. 10 Log characters and the DST test results of HSS-1.

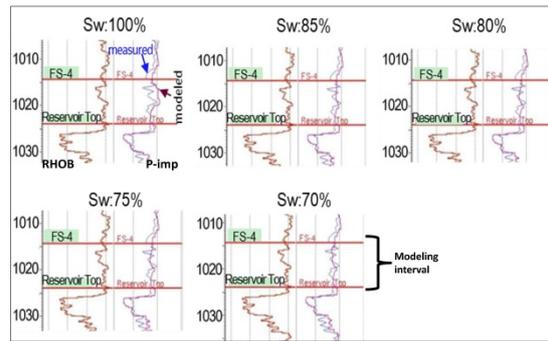


Fig. 11 The rock physics modeling and fluid substitution applied to the silty sand right above the producing zone in HSY-4 well.

## Conclusions

Two Plio-Pleistocene biogas systems were identified in this study. The freshwater biogas system distributes in the Annan-Chiku area in the Tainan and upper Liushung formations. The source rocks are mud/shale deposited in marsh/lagoon with TOC value ranges from 0.3-0.885%. Temperature for maximum biogas generation probably plays an important role in evaluating the resource potential. Sand control technique will be the key issue in future biogas exploration and development. The marine biogas system is mainly associated with the Plio-Pleistocene submarine canyon systems and distributes in the eastern part of the Chianan plain. Three types of play were analyzed and supported directly by the mud log anomalies. Conventional stratigraphic trap combined with residual gas was proposed for the biogas trapping mechanism of the sweet zone of LS\_A f 10 KM<sup>2</sup>. HSY-8 well drilled in late December 2017, accidentally proved the potential of the sweet zone of the lower ECS play.

## Acknowledgement

This research was supported by the petroleum foundation, ministry of economic affair of Taiwan through grant 106—F0105 to EDRI, CPC Corporation, Taiwan.

## Reference

Berkenpas, P.G., 1991. The Milk River shallow gas pool: Role of the updip water trap and connate water in gas production from the pool. in SPE Annual Technical Conference and Exhibition, Society of Petroleum Engineers. Chen, W.S., Ridgway, K.D., Horng, C.S., Chen, Y.G., Shea, K.S., and Yeh, M.G., 2001. Stratigraphic architecture, magnetostratigraphy, and incised-valley system of the Plio-Pleistocene collisional marine foreland basin of Taiwan. *GSA Bulletin*, v. 113, no. 10, p. 1249-1271. Fuh, S.C., Chern, C.C., Liang, S.C., Yang, Y.L., Wu, S.H., Chang, T.Y. & Lin, J.Y., 2009. The biogenic gas potential of the submarine canyon systems of Plio-Pleistocene foreland Basin, southwestern Taiwan, *Marine and Petrol. Geol.* v. 26, p. 1087-1099. Fuh, S.C., Liang, S.C., and Wu, M.S., 2003. Spatial and temporal evolution of the Plio-Pleistocene submarine canyons between Potzu and Tainan, Taiwan. *Petrol. Geol. Taiwan*, v. 36, p. 1-18. Hsu, L.M., 1984. Pleistocene formation with dissolved-in-water type gas in the Chianan plain, Taiwan. *Petrol. Geol. Taiwan*, v. 20, p. 199-213. Huang, Yu-Ting., 2001. Upper Quaternary Sedimentary Environments and Sequence Stratigraphy of the Tsengwen-hsi River Basin, Chianan Plain : A Preliminary Study . Master thesis of National Taiwan University, 187 P. Huang, Wei-Cheng., 2010. Stratigraphic sequences in distal part of foreland basin in southwestern Taiwan: Model of interplay between tectonic and eustasy. 126 P. Master thesis of National Cheng Kung University. Kallmeyer, J., and Wagner, D. (eds.) , 2014. Microbial life of the deep Biosphere, De Gruyter GmbH, Berlin/Boston, p.264-265. Li Y. L. and Lin, C. M. (2010) Exploration methods for late Quaternary shallow biogenic gas reservoirs in the Hangzhou Bay area, eastern China. *AAPG Bulletin*, v. 94, n. 11 (November 2010) p. 1741-1759. Mendell, P., 2012. The biogenic gas potential of Taiwan's coastal plain. A proposal to CPC Corporation, Taiwan. Schneider, F., Dubille, M. and Montadert, L., 2016. Modeling of microbial gas generation: application to the eastern Mediterranean "Biogenic Play". *Geologica Acta*, v. 14, no. 4, p. 403-417.

## 附錄 – 短期課程課堂筆記內容

2018 SE9.

short course.

專題名稱: Structural Geology in Seismic Interpretation

天氣: 雨.

專題案號: Shankar Mitra  
School of Geology and Geophysics  
University of Oklahoma

日期: 2018年10月13日 星期: 六.

17:00 下课

1. Introduction

If seismic data is not perfect...

震測成像不完美(常見)的狀況下

→ 如何應用震測解釋、建立地質模式。⇒ 本課程的目的。

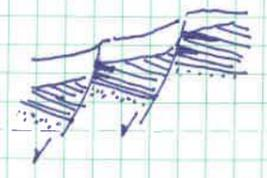
• 一般進入礦區, 會先探尋構造封閉。

在震測解釋之前需先了解:

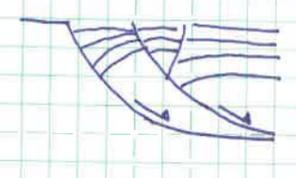
1. 震測解釋, 在資料不好的區域, 可能難以得到好的解釋結果。
2. 構造模型(概念), 對於進行 2D, 3D 資料解釋 (特別是資料不佳區域), 具有引導、指導的作用。
3. PSDM 資料處理前的構造概念, 可能影響 PSDM 的構造型態。
4. 解釋時, 需符合平緩地質的概念。

• 相同的 tectonic regimes, 可能具有相同且重覆出現, 並能將一樣的概念應用於構造型態的盆地/區域。

• 相同的應力環境, ex. extensional fault 會有不同的構造型態、斷層、油藏位置。



basement involved



detachment.

↓  
解釋前, 需先了解 structural concept!

• Mechanical Stratigraphy

→ Mechanical stratigraphy refers to the subdivision of stratigraphic units based on their mechanical properties!

→ 一樣是 compressional system. 岩性的差異, 造成構造上的差異.

Canadian Rockies.

carbonate. 上覆厚 shale

許多逆斷層.

主要層層為 carbonate

Wyoming overthrust belt.

侏羅 → 白堊

s.s. sh. carbonate carbonate.

許多 fold

主要層層為 s.s.

make multiple possible interpretation before make the conclusion.

震測解釋時, (特別是當資料, 斷層處), 儘量做出不同的構造型貌解釋.

並討論各種型貌的可能性.

→ 不同的構造型貌, 其油藏的型貌, (位置可能不同).

專題名稱:

專題案號:

同P57

天氣: 雨

日期: 2018年10月13日 星期: 六

2. Common Pitfalls in Seismic Interpretation Structures.

• 許多解釋人員在解釋時, 常會將拿到地震測資料當成是真實地質狀態, 而忘了去查看速度資料是否合理. (特別是深度域移資料!)

比較 unmigrated data ↔ migrated data

Pull up 現象, 若速度資料正確, 應會完全消除, 但一般很難辨別.

Pushdown

PSDM 資料, 很難分辨 pull up 現象是真實, 還是速度分析上到不準確?!

Push down

模型

• Seismic Pull ups & Pushdowns

\* Pull ups.

→ Thrust Thrust Reverse faults and folds

→ Subsalt - Autochthonous

→ Reefs

\* Pushdowns

→ Normal faults - fault shadow effects.

→ Salt in carbonate sections

→ Channels and surface effects

→ Low velocity layers.

• Migration Related Pitfalls.

→ Migration of single reflectors or diffractors can lead to Trail or Noise along migration paths.

→ Incorrect velocities used in either Post-stack or Pre-stack Migration can lead to Migration Trails or "smiles" or "frowns".

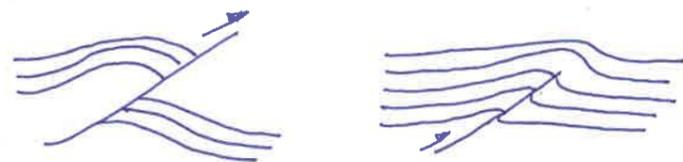
→ Structural Models necessary for seismic processing (ex. PSDM)

→ Wrong Models leads to incorrect processing and interpretation.

• Bad migration doesn't mean the bad job of data processing.

→ Velocity 不夠準確. 且總是有不準確的可能.

⇒ 解釋人員需注意不同資料其移位 (migration) 上的影響



faulting and steep limbs both result in similar images!!!  
斷層或陡峭的褶皺可能產生相同影像。

在 PostStack Depth Migration 或 Time Migration 資料上. 此兩種構造型貌. 都可能產生一樣的 seismic migrated profile.

⇒ 如何做決定?

- 比較其它鄰近相同/類似型貌的構造.
- 風險評估.

• Display Related Pitfalls.

→ Necessary to Display Time or Depth Profiles on one to one scale (no vertical exaggeration)

展示實際比例的震測資料. 以免對構造有錯誤的認識!

專題名稱:

專題案號:

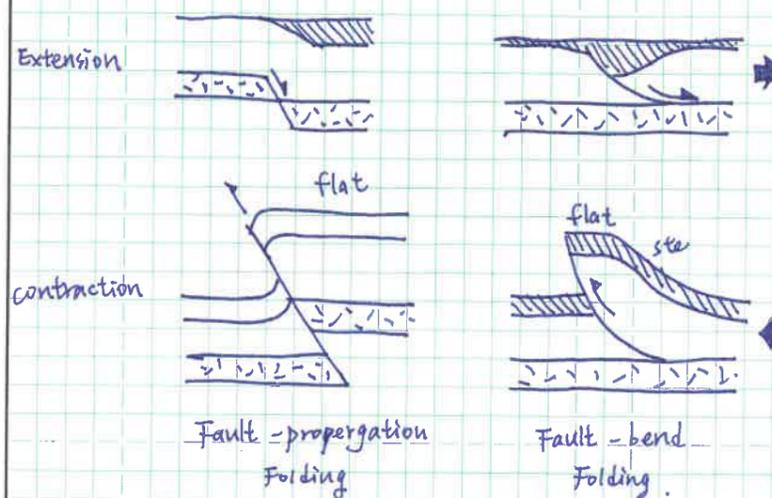
同 P57

天氣: 雨

日期: 2018年10月13日 星期: 六

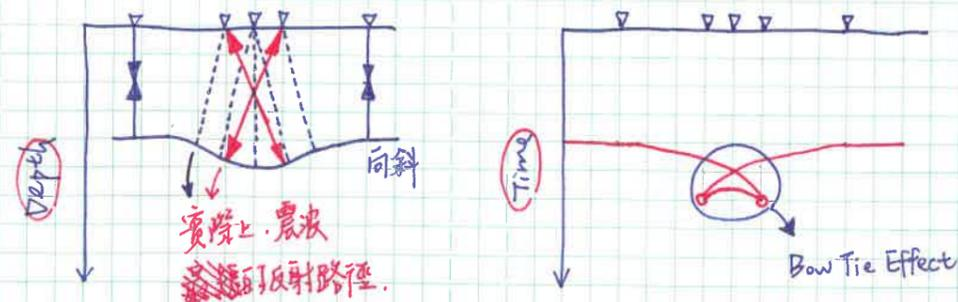
3. Seismic Expression of Folds, Faults, and Unconformities.

Fault-related Folds. { Fault-propagation Folding  
Fault-bend Folding

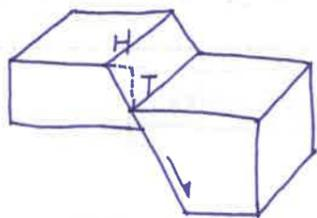


• "Bow Tie Effect" in syncline.

Move out { under migration  
over migration } in anticline



• Dip Separation



H: Heave. 斷層橫斷距. 斷距. 斷層落差.  
 T: Throw. 斷層縱斷距. 斷層平錯. 蒙反了

• Seismic Expression of Faults

pp. 111

→ 斷層面的反射一般多來自於低角度斷層. 如: Listric Growth Faults, Thrust Faults.

→ 斷層面兩側的岩性需有差異 (R.F), 才能有反射信號.

→ 一般多藉由觀察. 層面的終止 (terminating) 和 offset (錯位).

需藉由正確的移位消除 diffractions.

lower or over migration, 可能造成斷層位置/角度上的錯誤定位/解釋.

• Mapping Faults Using Coherence Data Volumes.

利用震測屬性. (若能知道區域的斷層位態) 可進一步加強斷層解釋的準確性.

ex. coherence, curvature,

a measure of similarity between waveforms and/or traces.

• Unconformities

- Disconformity
- Non-conformity
- Angular unconformity

專題名稱:

專題案號:

同P57

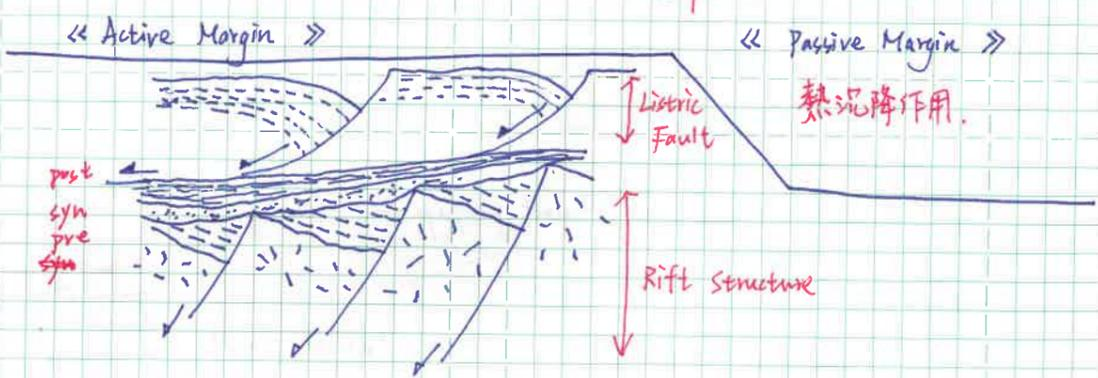
天氣: 雨

日期: 2018年10月13日 星期: 六

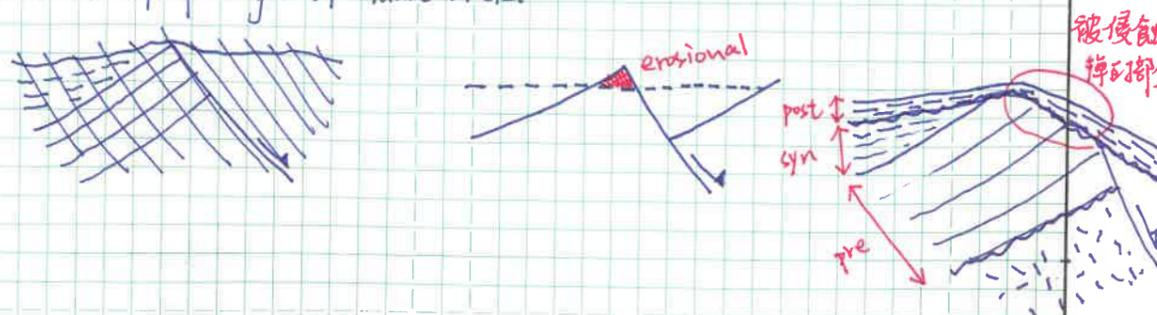
4. Extensional Structures.

包含 Rift Structures

Listric Growth Faults.



• Erosion of Updip Edge of fault block.



● 斷層成像問題

1. 斷層角度, v.s. 地層傾斜.

2. Fault Shadow Under Normal fault.

Seismic Pushdown.

斷層斷距越大 → 斷層兩側速度差異越大 → Pushdown 越明顯.

Drape

● ~~Drag~~ Fold.

→ Active ~~Drag~~ Drape } Transfer of fault slip to folding in overlying strata  
 Extensional fault-propagation folding.

→ Passive ~~Drag~~ Drape

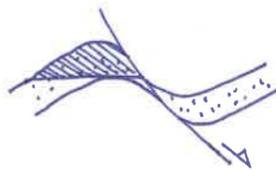
Differential compaction above buried fault



斷層兩側地層  
沒有 ~~drag~~ Drape  
是否有油藏, 決定  
於斷層封阻能力



斷層兩側地層  
有 ~~drag~~ Drape  
但斷層無封阻  
則封閉只限於  
Drag fold 未被斷層  
截穿部分.



斷層兩側地層  
有 ~~drag~~ Drape  
斷層有封阻  
封閉面積可能很大.

專題名稱:

專題案號:

同 P57

天氣: 雨

日期: 2018年10月13日 星期: 六

● 如何識別震測資料上, Pushdown 和 ~~Drag~~ Drape Fold?

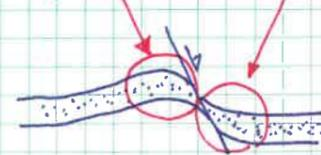
\* Unfaulted Drape Folds

→ 成像良好.

\* Faulted Drape Folds

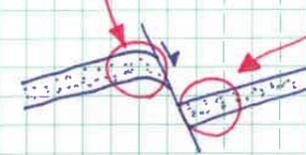
→ 震測影象品質可能隨不同地質狀態, 斷層型貌有所差異.

→ 若下盤 downwarp 且上盤 turn up, 則 faulted Drape Fold 型貌可能失真.



由於上盤的 turn up 並不總能完美/良好地成  
像, 因此, 若真的看到上盤 turn up, 極有  
可能真的是 Drag fold.

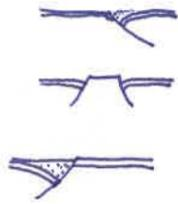
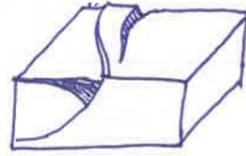
→ 若僅有下盤有 downwarp 現象, 上盤沒有, 則可能是受到橫向速度差異  
所引起的 fault shadow effect (即 push down)



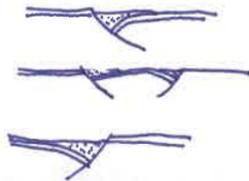
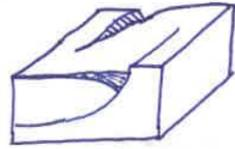
→ Downwarp in successive beds is vertically stacked for a seismic push down.

• Transfer zone

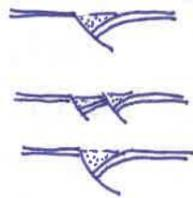
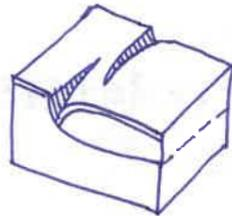
Divergent



Convergent



Synthetic



此處的 Divergent, convergent, synthetic 指的是各正斷層間的傾向和相對位置關係。

專題名稱：

專題案號：

同 P57

天氣：雨

日期：2018年10月13日 星期：六

5. Extensional Structures - Listric Growth Faults

在 Passive Margin, shelf edge (sediment wedge) 會隨 { 沉積速率, 構造沉降.

的影響, 漸往外發育. ex. 墨西哥灣北側. Lower Cretaceous shelf edge.  
↓  
現今的 shelf edge.

• Listric Growth Faults.

→ Homogeneous sequence

Long fault systems, dipping basinward, ~~still~~ striking parallel to the present coast, and NOT associated with near surface salt structures.

→ Ductile Basal layer (ex. salt 鹽)

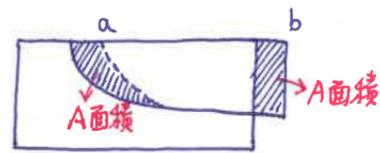
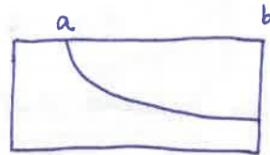
Shorter, more arcuate fault systems, dipping landward and basinward and associated with abundant near-surface salt structures.

P5, P7.

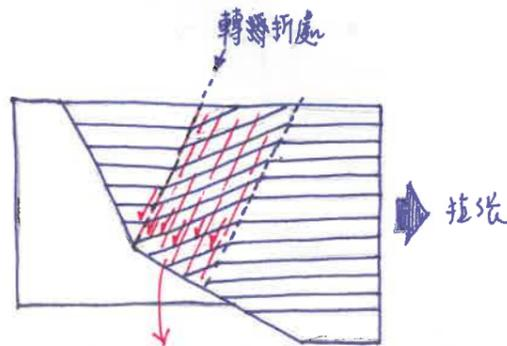
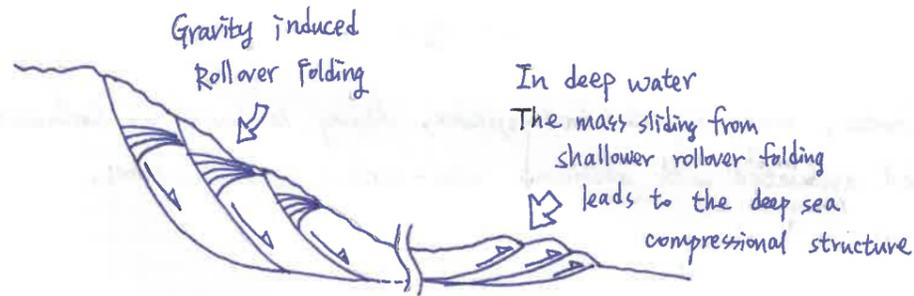
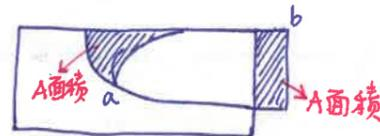
• Mechanism of Rollover Folding

- Fault-Bend Fold Theory
- Antithetic Fault and Rollover
- Synthetic Fault and Drapes

\* Rollover Folding 的平衡剖面 / 概念 (Area-balanced model)



兩位置的A面積都相同。



隨著拖張的發育 (Listric 的發育) 在轉折處會發育斷距很小的 Antithetic 斷層。每個 antithetic fault 會被保留於地層中。

這些 antithetic faults 或許於震測資料上顯示不出。但常於鑽井記錄上被發現。

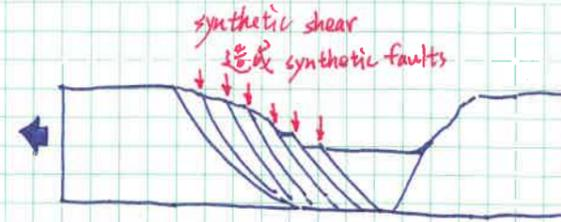
專題名稱：

專題案號：

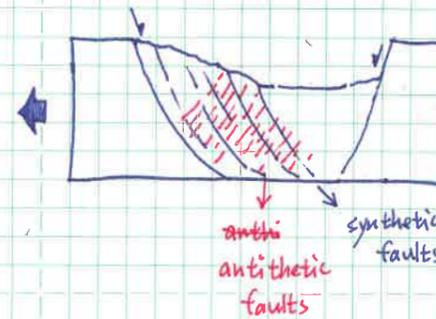
同 P57

天氣：雨

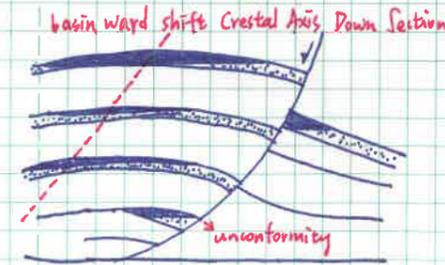
日期：2018年10月13日 星期：六



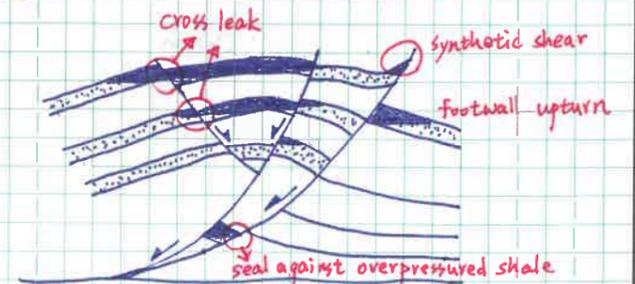
綜合 antithetic 和 synthetic faults 於 Listric Fold 上。會造成以下斷層分佈



\* Structural Trap Styles. 封閉類型



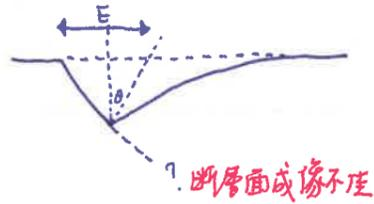
Rollover Fold and Unconformity or pinchout



Rollover Fold and Fault

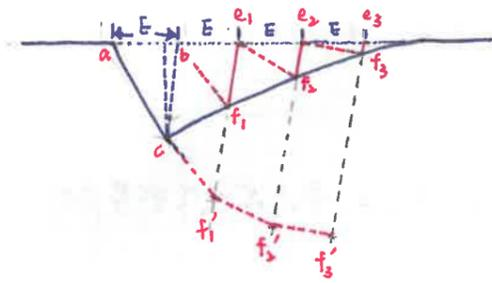
Modeling Fold-fault Geometries.

\* 利用已知的 Roller anticline 影像. 推測其它部分. (Inclined shear)



theta 為 antithetic 和 垂線 的 角度.

斷層面 成 像 不 佳



1. 自 b 點 往 背 斜 頂 端 (右 側) 間 隔 描 繪 等 間 距  $\overline{ab} = E$ .
2. 自 每 個 e 點. 繪 製 平 行  $\overline{bc}$  線 段 之 平 行 線.
3. 連 結 並 繪 製  $\overline{bf_1}$ ,  $\overline{ef_2}$ ,  $\overline{ef_3}$ .
4. 繪 製 不 同 區 段 的 平 行 四 邊 形. 依 序 標 示  $f_1'$ ,  $f_2'$ ,  $f_3'$  的 位 置. 則 可 得 到 推 測 出 的 斷 層 面  $\overline{cf_3}$  位 置.

- 此 圖 表 示 基 本 假 設
- Constant Heave
  - Constant Displacement
  - Constant Line Length.
  - Inclined Shear

730

專題名稱:

天氣: 雨

專題案號:

同 P59

日期: 2018 年 10 月 13 日 星期: 六

6. Salt and Shale Structures

◎ Salt composition:  
→ Salt 為 一 種 蒸 發 岩 (evaporite)

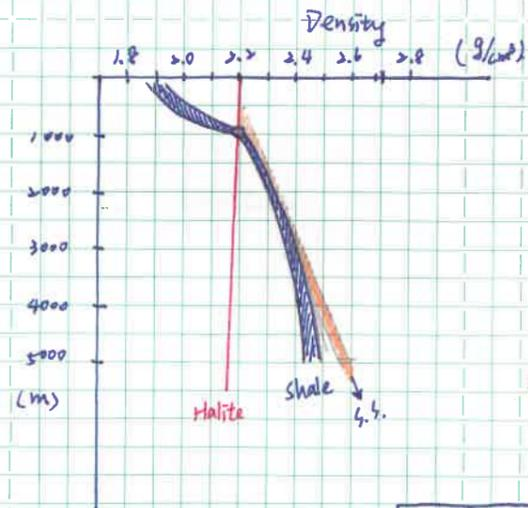
Anhydrite flow less than Halite

溫/壓 對 流 變 和 密 度 的 影 响

pressure <sup>increasing</sup> ~~increasing~~ with depth. → decreasing volume, increasing density

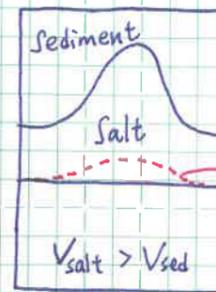
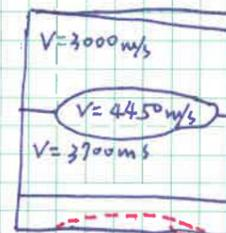
temperature increasing with depth → increasing volume, decreasing density

• Salt 在 3~4000 feet 深 時. 開 始 可 移 動. 因 為 大 概 在 此 深 度 以 下  $\rho_{salt} < \rho_{gs}$  或  $\rho_{sh}$ .



	Density	Velocity	
岩 鹽	Halite	2.17	4500
硬 石 膏	Anhydrite	2.98	6000

(m/s)

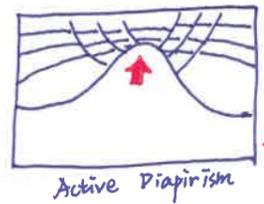


因  $V_{salt} > V_{sed}$ . 故 於 震 測 剖 面 上 造 成 seismic pull up 現 象.

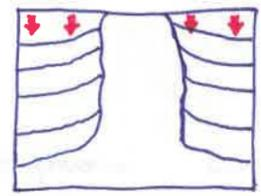
Mechanisms of Salt Diapirism.

傳統上，區分為 Active Diapirism 和 Passive Diapirism

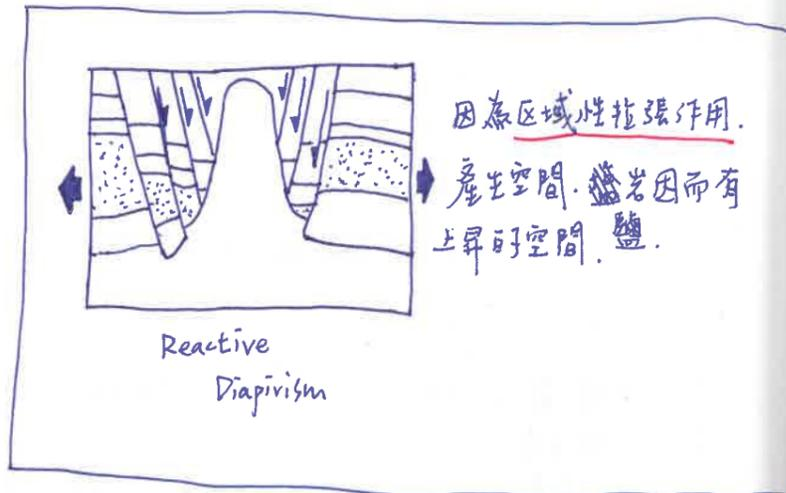
但是近來，普遍認為大多作用都是 Passive Diapirism。



鹽岩上升使得上方地層產生破裂。



因地層沉降而使得鹽岩上升



因為區域性拉張作用，產生空間，鹽岩因而有上升的空間。

allochthonous 移置的  
autochthonous 原生的

piercement 穿頂的 piercement salt dome 穿頂鹽丘

canopies, canopy 有蓋，有罩的

2018 SEG short course

專題名稱: Structural Geology in Seismic Interpretation

專題案號: Shankar Mitra

天氣: 陰

日期: 2018年10月14日 星期: 日

Modeling of Passive Diapir By Stiff Overburden

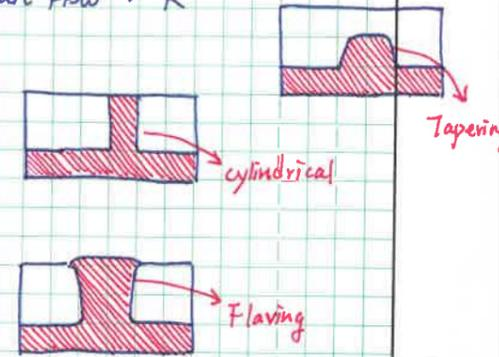
Sediment loading : A

The Rate of Salt Flow : R

→ Tapering Regime =  $R/A < 1$

→ Cylindrical Regime =  $R/A \approx 1$

→ Flaring Regime =  $R/A > 1$



$R/A$  increase, means increasing of salt flow.

Factors controlling salt Flow Rate 控制鹽岩流動速率的控制因素

- 1: Sedimentary Load
- 2: Sedimentation Rate
- 3: Thickness of salt Layer.

\* 沉積速率慢 ( $R/A < 1$ )，為 Passive Diapirism 的產生原因。

\* 若鹽丘埋深沒有很深，則鹽丘自身的浮力，可能於頂部地層產生正斷層，作為沉積上發育的通道。(active process)

\* <sup>埋深</sup>少於 2000 呎 (約 1000m)，有拉張作用產生正斷層，製造岩鹽能進入的空間，則會隨地岩鹽向上發育、移動。(active process)

• Salt Pillows and Diapirs

P20

→ Pillows (Non-piercement piercement) 非穿頂鹽丘. - Primary Rim Synclines  
主要沿巨外緣向斜.

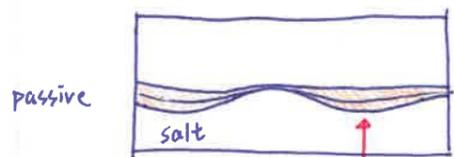
→ Diapirs (piercement?) 穿頂丘? - Secondary rim syncline, Turtle structures  
次要(=次)沿外緣向斜. 龜背構造

→ Bubs & Teardrops 燈炮型. 淚滴型

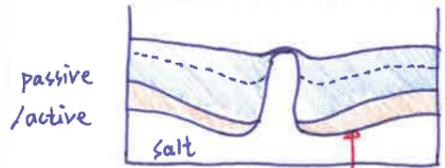
→ Canopies 有蓋. 有罩的

→ Salt sheets & Tongues

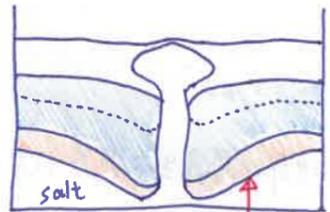
• Evolution of Salt Diapirs



向斜



背斜 Turtle Structure



背斜 Turtle structure

→ 由向斜轉換為背斜.

專題名稱:

專題案號:

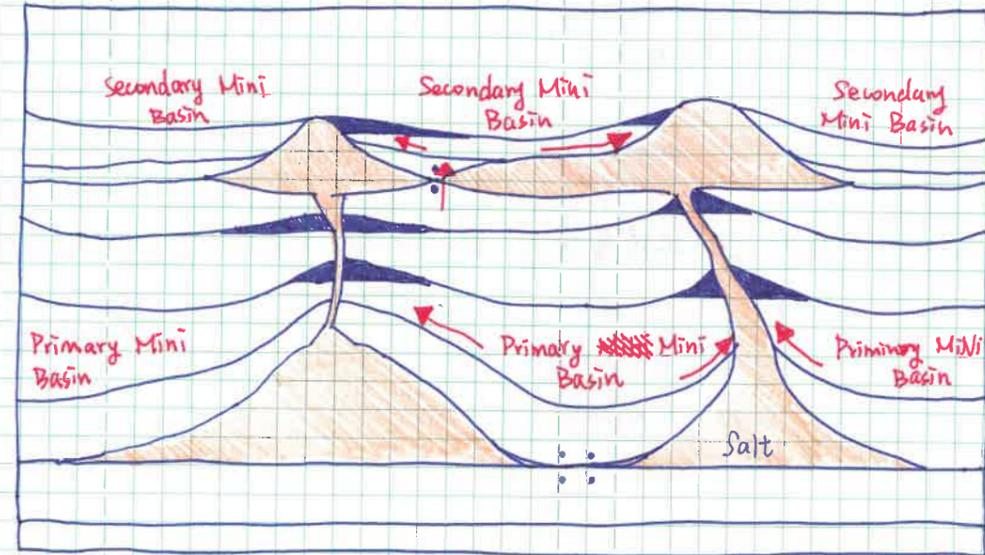
同 P65

天氣: 陰

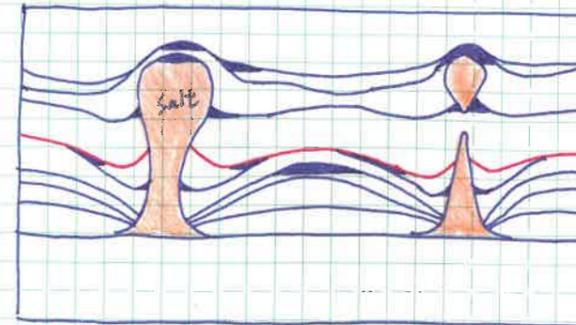
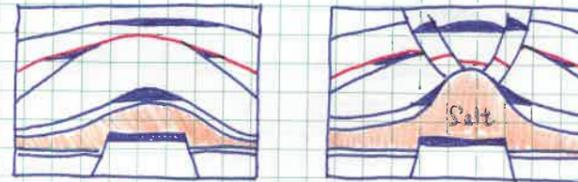
日期: 2018年10月14日 星期: 日

P29

• Minibasin



• Salt ~~rela~~ - Related Structural Traps

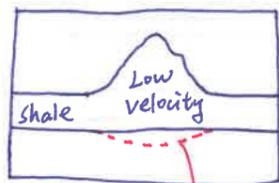


② Shale Tectonic

- Shale is most mobile when overpressure at depth of approximately 10,000 ft
- Dewatering leads to reduction in shale mobility
- Reburial may lead to increase in mobility.
- Internal processes such as release of water through diagenesis (smectite-illite) (膨潤石的伊蒙石化是深埋時常見的礦物學反應) or generation of hydrocarbons (油氣生成) increases mobility → volume increases by a few percent. 成岩作用或油氣生成會增長 shale 的流動性。
- Therefore, shale deformation may be more episode during major overpressuring effect.

\* shale 的 Density ( $\rho$ ) 和臨近的沉積層相近, 因此 shale 的頂底不會有強反射。

↓  
salt 頂底則有



因此 overpressure 造成  $V_{shale}$  較低。  
因此於震測剖面上, 會於 shale 底部造成 Push down 現象

專題名稱:

專題案號:

同 P65

天氣: 陰

日期: 2018 年 10 月 14 日 星期: 日

7. Compressional Structures - Fold and Thrust Belt

- Controls of Mechanical Stratigraphy on structural styles.

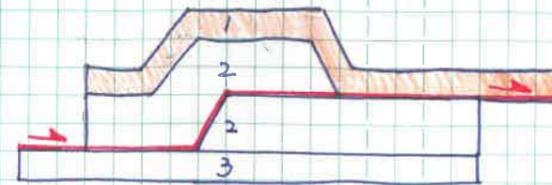
- Fault-Bend Folds
- ~~Detachment Folds~~ Fault-Propagation Folds
- Detachment Folds

a. Fault-Bend Folds

→ Many thrust faults are characterized by a stair-step trajectory, in which the fault follows bedding parallel detachments in incompetent units and climbs through more competent unit along ramps.

→ Movement of the thrust sheet over each ramp produces a rootless ~~supp~~ anticline and passive synclines.

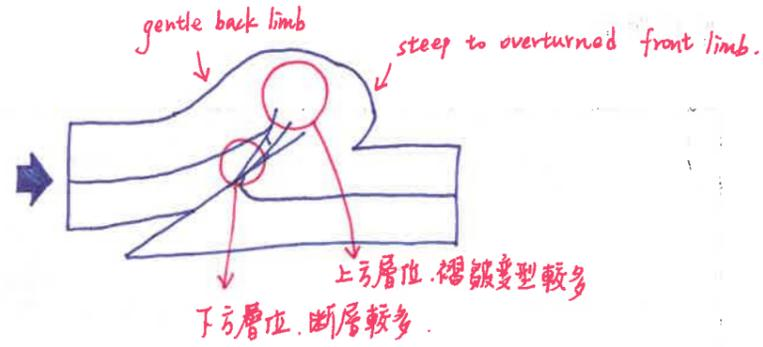
→ The model was first proposed by Rich (1934) to explain the formation of the Powell Valley anticline and the Middlesboro syncline as a result of the movement on Pine Mountain thrust.



Normal stratigraphic sequence	older beds thrust over younger beds	Normal stratigraphic sequence
Thicken Thickness normal	Section Thickened by Duplication of beds	thickness normal

b. Fault - Propagation Folds

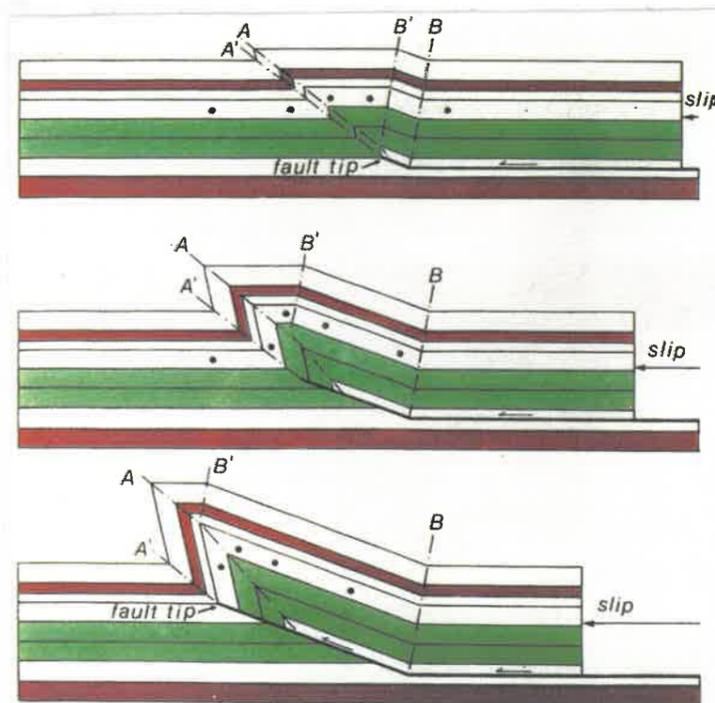
1. 由平緩的後翼和陡峭前翼所組成
2. 斷層逐漸往前丟失位移量，最後終止
3. 褶皺的大小和斷層的滑移量有關



4. 基本上，要造成 Fault-propagation folds，地層需由許多相對的質的薄互層所組成 (thin-bedded multilayers)

5. 撓曲及滑移 (Flexural-slip) 是主要的變形機制 (deformation mechanism)

• Self-Similar Fault-Propagation Fold.



$\overline{AA'}$ 、 $\overline{BB'}$ 、 $\overline{AB'}$  角度維持不變。  
沒有下盤的傾斜存在。

專題名稱：

專題案號：

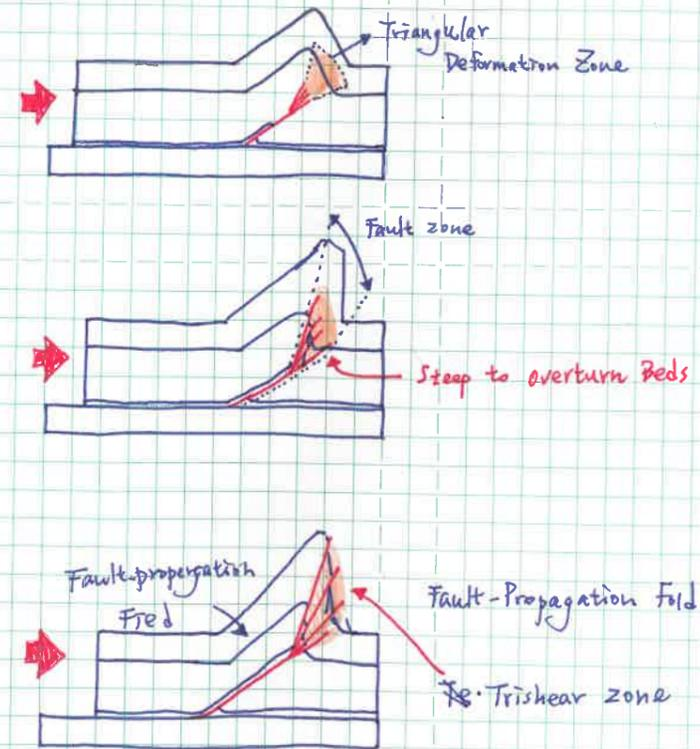
同 P65

天氣：晴

日期：2018年10月16日 星期：日

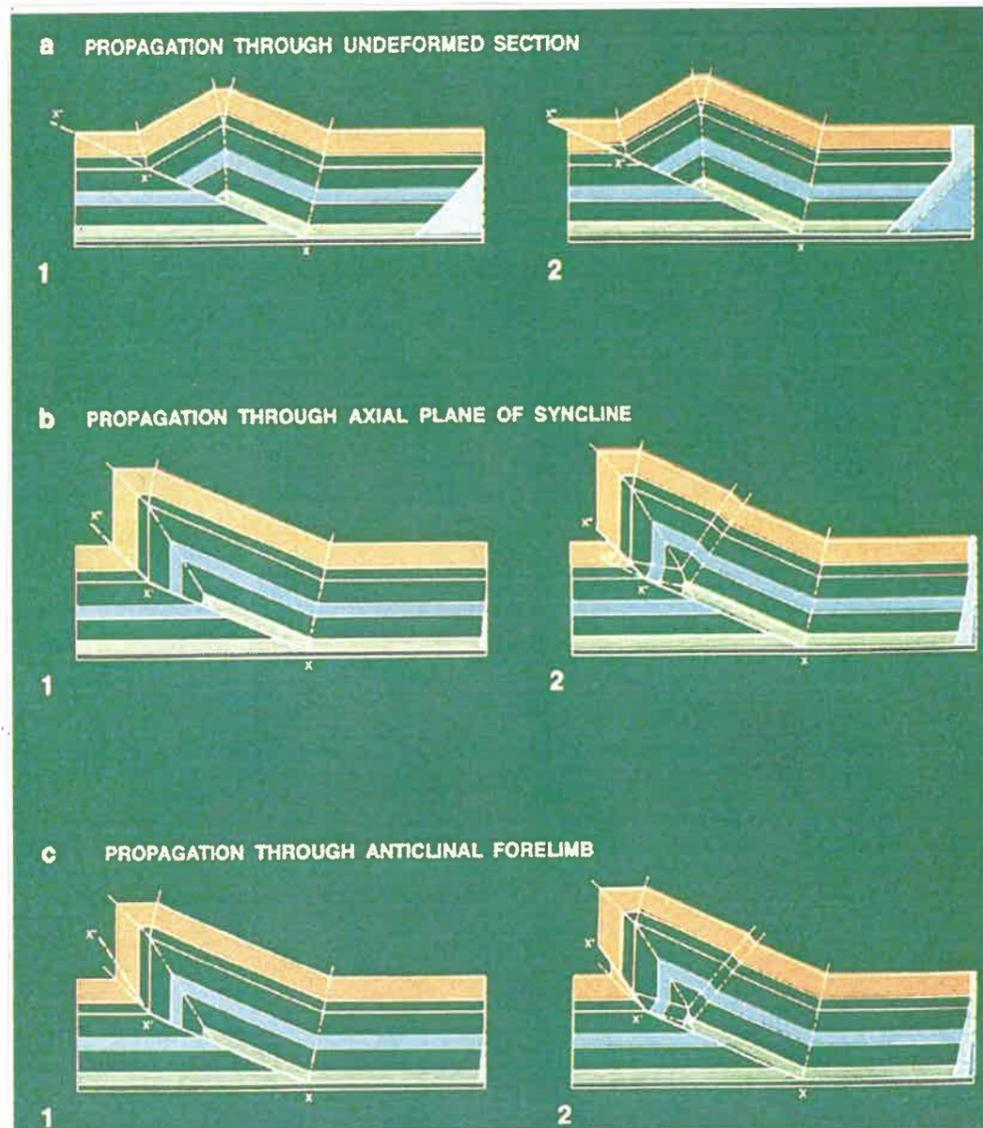
• Trishear Fault-Propagation Model

1. 斷層的滑移量於三角帶變形 (triangular deformation zone) 處逐漸消失，隨著變形的演進，發生剪應變。
2. 三角剪切帶 (trishear zone) 由覆瓦狀排列 (imbricate) 的逆斷層所組成。
3. 根據此模型，褶皺前翼 (forelimb) 於一開始先增厚，隨著擠壓持續進行逐漸變細。
4. 褶皺前翼的傾角隨變形漸增加。



Translated Fault-Propagation Folds

P23



PART III CLASSES OF STRUCTURES

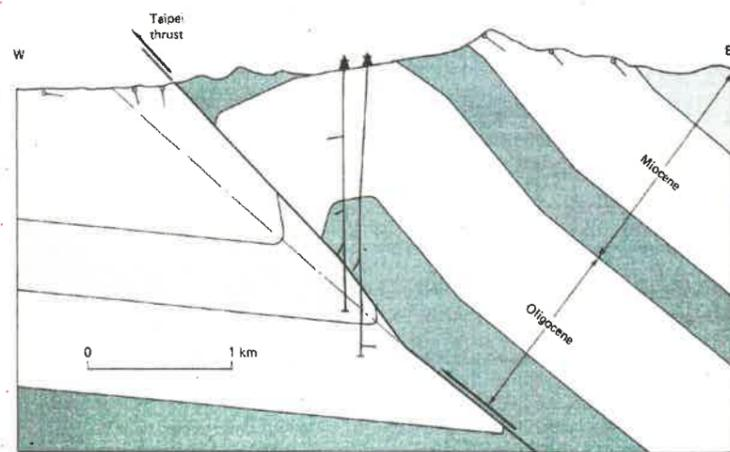


FIGURE 9-49 Cross section of broken fault-propagation fold along Taipei thrust, western Taiwan.

專題名稱：

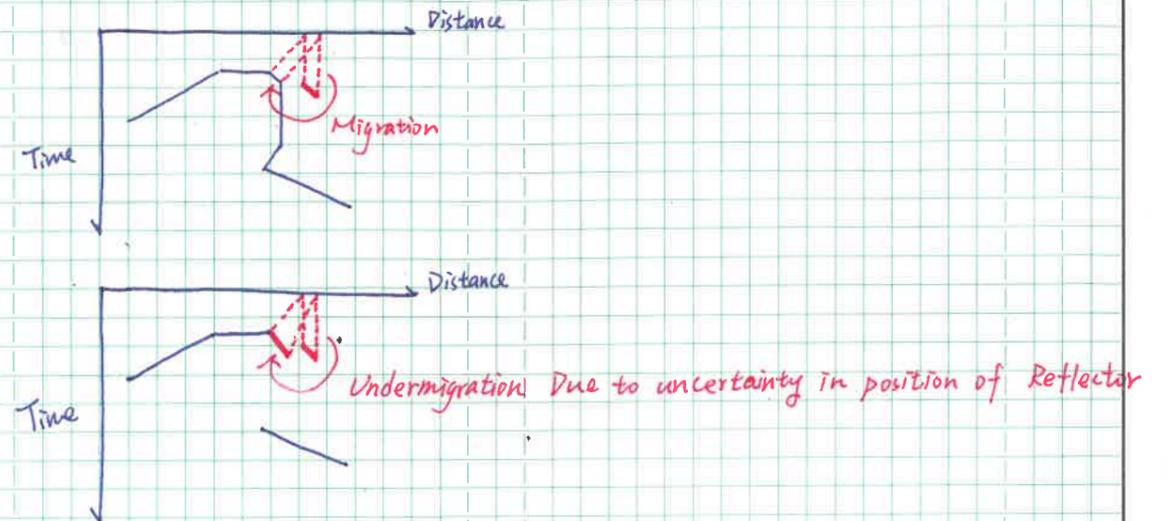
專題案號：

同 PG5

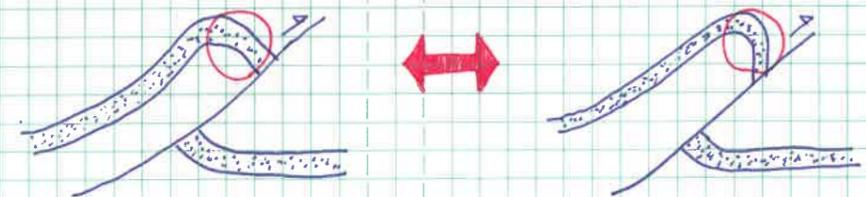
天氣：陰

日期：2018年10月14日 星期：日

\* 褶皺前翼的角度因太陡/或倒轉，所以難以震測成像。



由於接收的不確定性/不準確性，使得震測剖面上，前翼的成像不清且位置不準確。



《震測成像》

《實際狀況》

Q: 要如何知道影像的正確與否? 或是否合理?

- 若能知道斷層的滑移量 (slip motion), 則能概略推測褶皺前翼的可能陡/緩。
- 滑移量大, 則前翼越陡。

P23

C. Detachment Folds

通常位於 Basal detachment plane 之上的為塑性地層. ex. salt, overpressure shale.

• Detachment Folds - Geometric Types.

→ Disharmonic Detachment Folds

Disharmonic detachment folds are characterized by parallel geometries in the outer layers, and disharmonic and non-parallel geometries in the lower unit with the folds terminating in a detachment.

Lift-off structures are characterized by tight isoclinal geometries of the upper unit, and a weak lower unit, which is isoclinally fore folded in the core of the anticline.

→ Lift Off Folds.

Lift-off structures are characterized by tight isoclinal geometries of the upper units, and a weak lower unit, which is isoclinally folded in the core of the anticline.

厚. 極為 Ductile 的 lower unit

易被褶皺的 upper unit.

P35

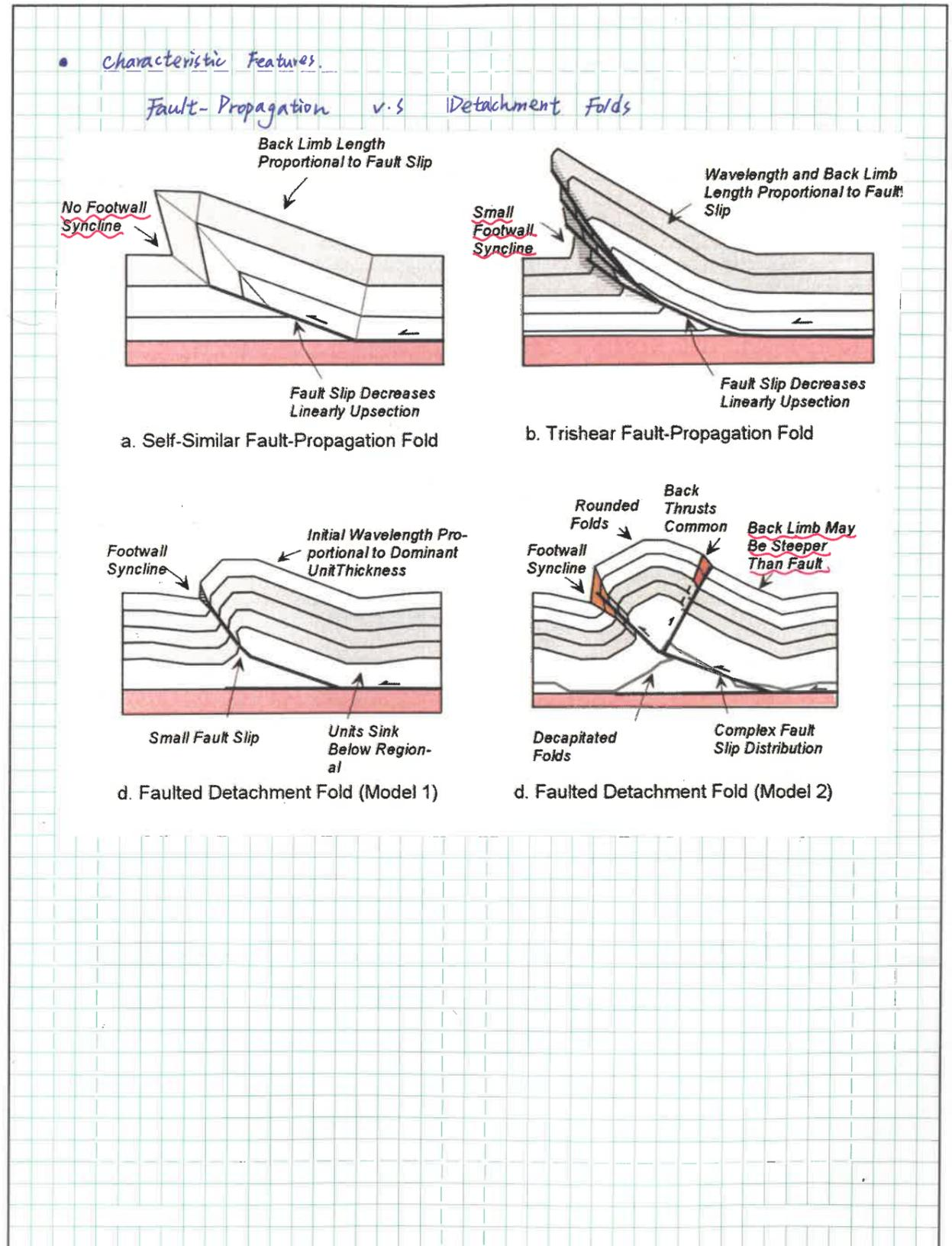
專題名稱:

專題案號:

同 P65

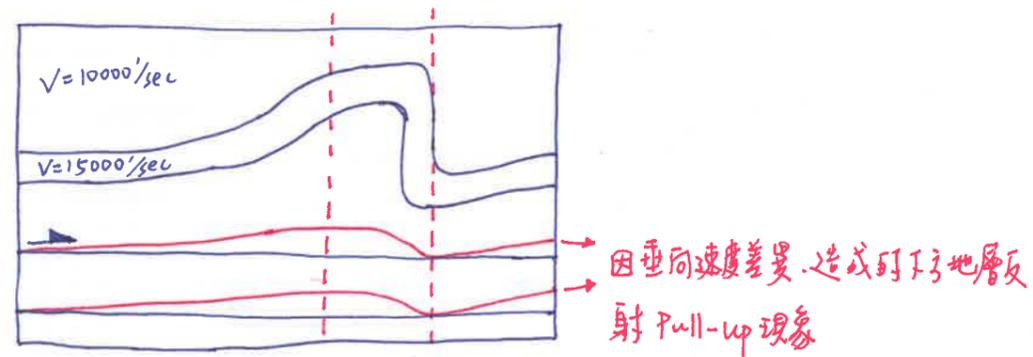
天氣: 陰

日期: 2018 年 10 月 14 日 星期: 日

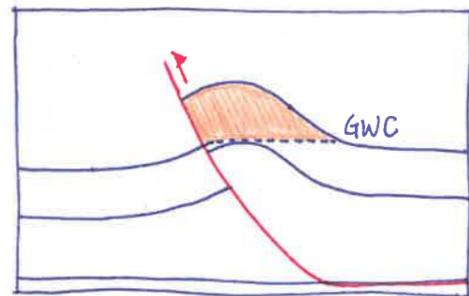


P47

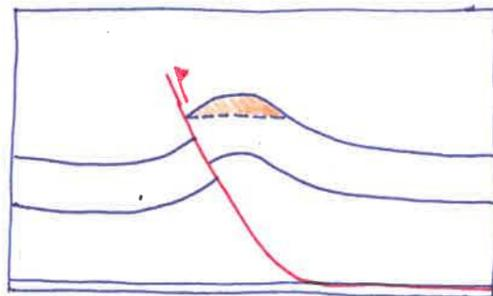
• Pull-Up of ~~Detach~~ Detachment and Underlying Reflectors



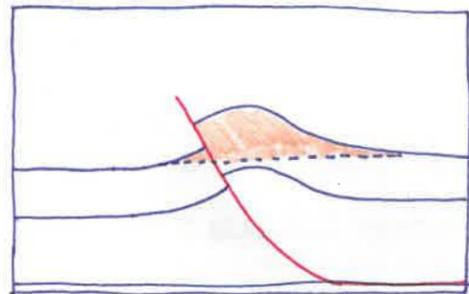
• Structural Closures in Fold-Thrust Structures



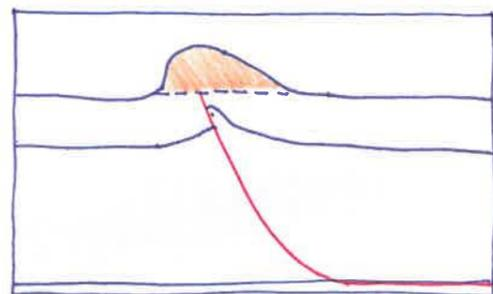
a. Sealing Fault



b. Dip-Leaking Fault



c. Cross Leaking Fault



d. Fold Closure

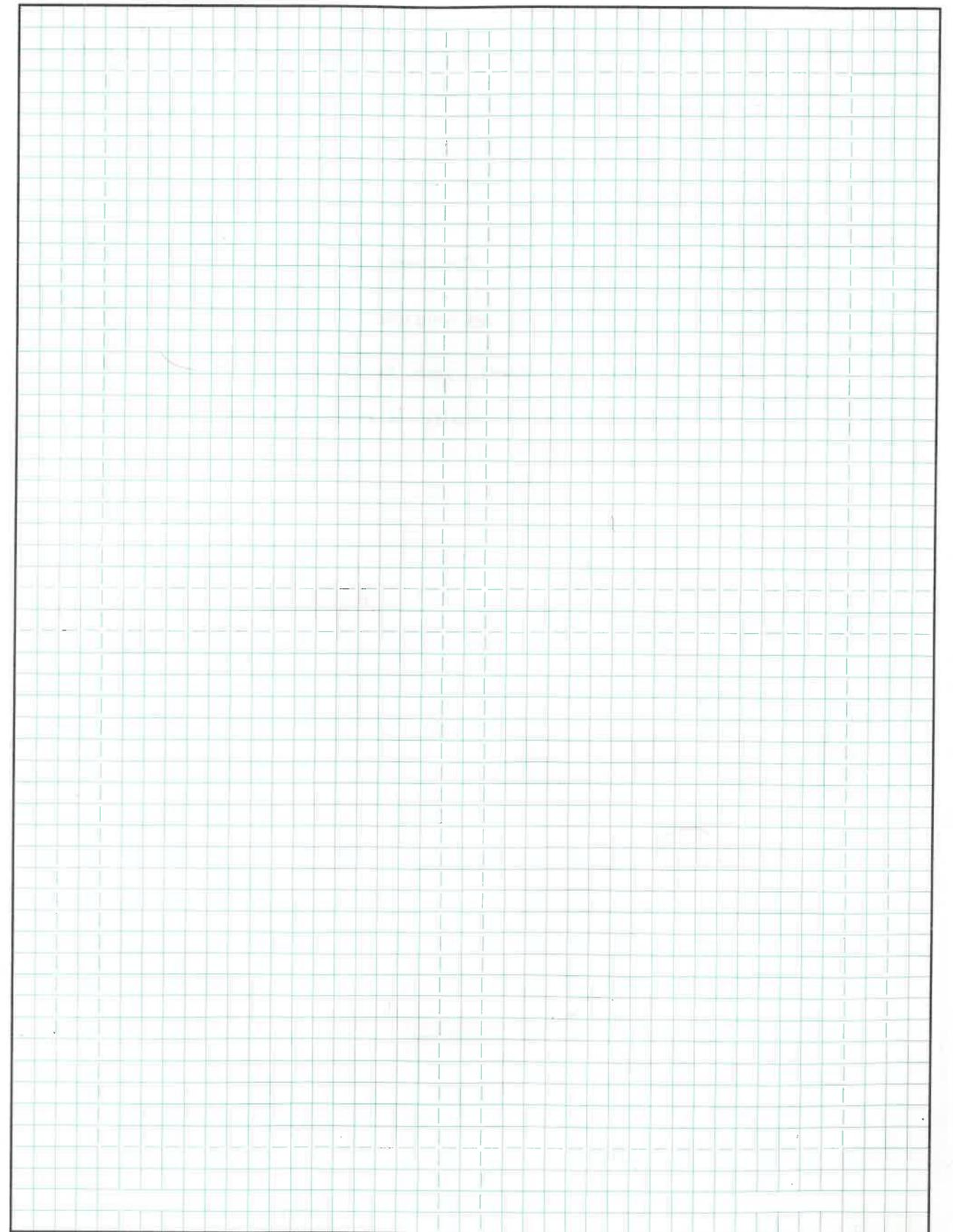
專題名稱:

專題案號:

同 P65

天氣: 陰

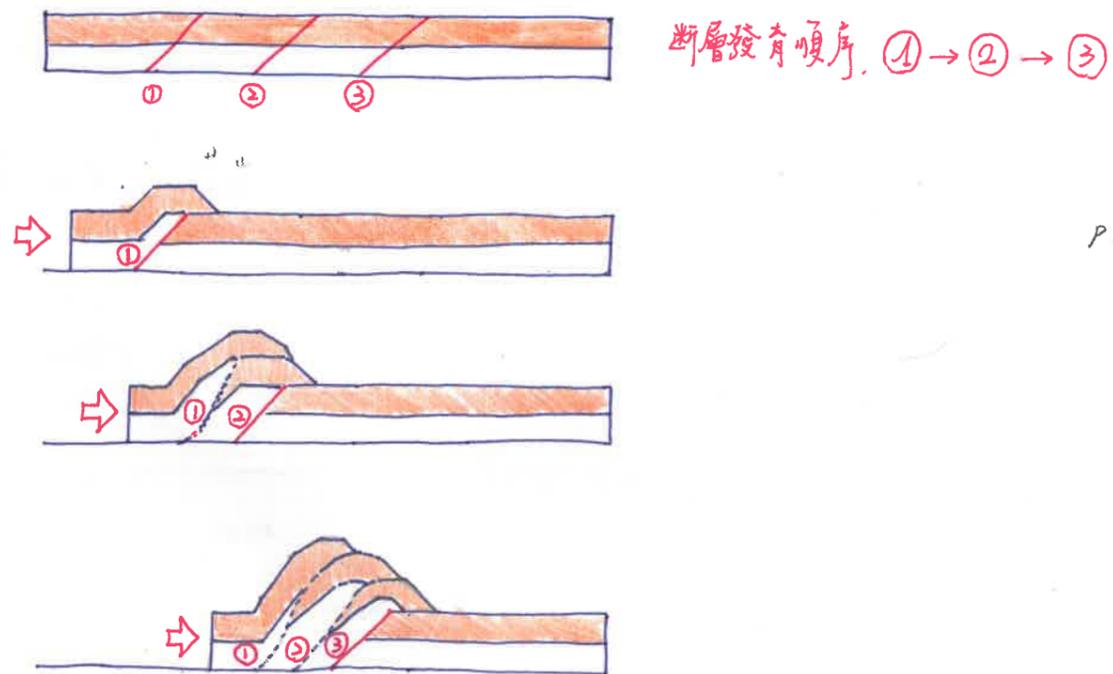
日期: 2018 年 10 月 14 日 星期: 日



● Fold - Thrust System.

\* Duplex Origin and Classification

- Initial slip results in the formation of a fault-bend fold due to movement of the hanging wall over a ramp.
- During movement on the next thrust, the earlier formed thrust and related fault-bend fold are folded.
- The successive formation of additional thrust results in a final structure made of multiple folded thrusts.
- The final geometry of the duplex structure is dependent on the initial spacing between the fault ramps and the ~~res~~ relative displacements on the faults.
- The interference of other structures, such as detachment fold, faulted detachment folds and fault-propagation folds results in other types of fold-thrust systems.



P21

專題名稱：

專題案號：

同P65

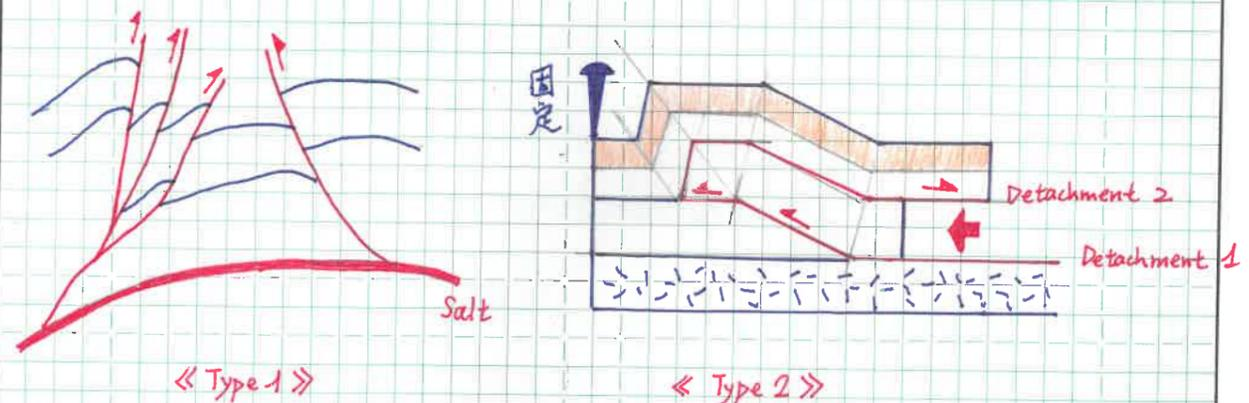
天氣：陰

日期：2018年10月14日 星期：日

\* Triangle Zones and Wedge Structures

→ Triangle zones

- Type 1 Triangle Zone → 具有相同的 Detachment
- Type 2 Triangle Zone → 具有不同的 Detachment



專題名稱：

專題案號：

同PG5

天氣：陰

日期：2018年10月16日 星期：9

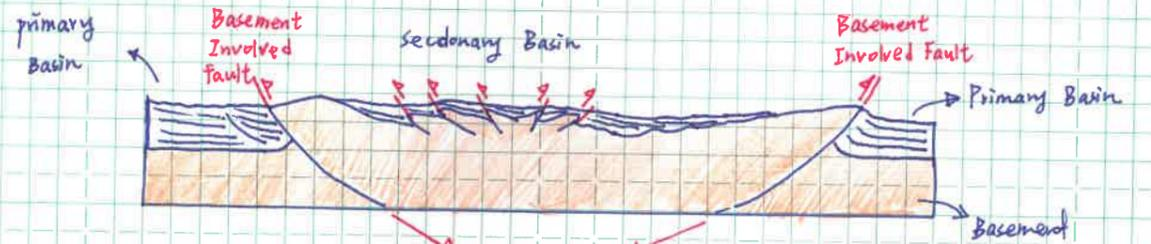
### 8. Basement - Involved Compressional Structures

一般常發生 / 常見於

此種構造型類通常連續性 / 延展性不佳，受控於 Basement 的型貌。

#### • Foreland Basement Structural Structures:

ex: Rocky Mountain, Laramide structures, central basin uplift, Wichita - Arbuckle Front, Andean Foreland - Sierras Pampeanas, Iberian Range, Spain, Atlas Mountain...



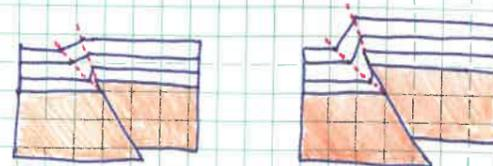
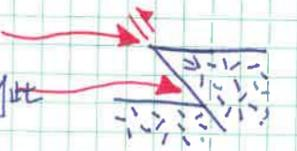
Basement Involved Fault  
Secondary Basin  
Basement

#### • 兩種 Basement - Involved 模型

1. Basement Faulted Model. 特點為基盤只有斷層，沒有褶皺。

上盤所造成之傾斜，其傾斜角線連結至上盤頂端

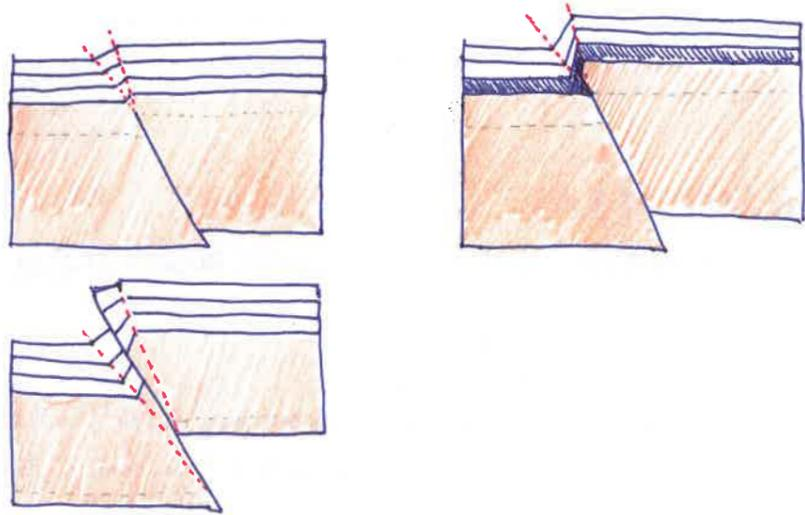
下盤所對應到之傾斜，其傾斜角線連結到此



Basement 自身沒有發生褶皺。

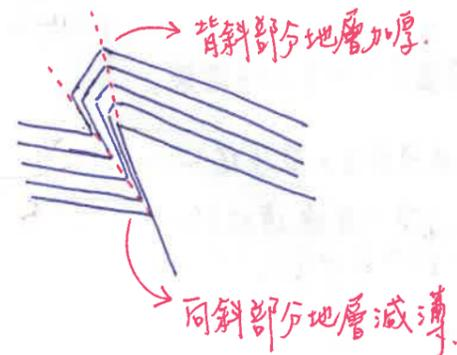
2. Basement Faulted and Folded Model.

此模型的特點是，斷層兩側的基盤具變形褶皺。



P10

• triangular shear zone 的特色.



P13

專題名稱：

專題案號：

同PG5

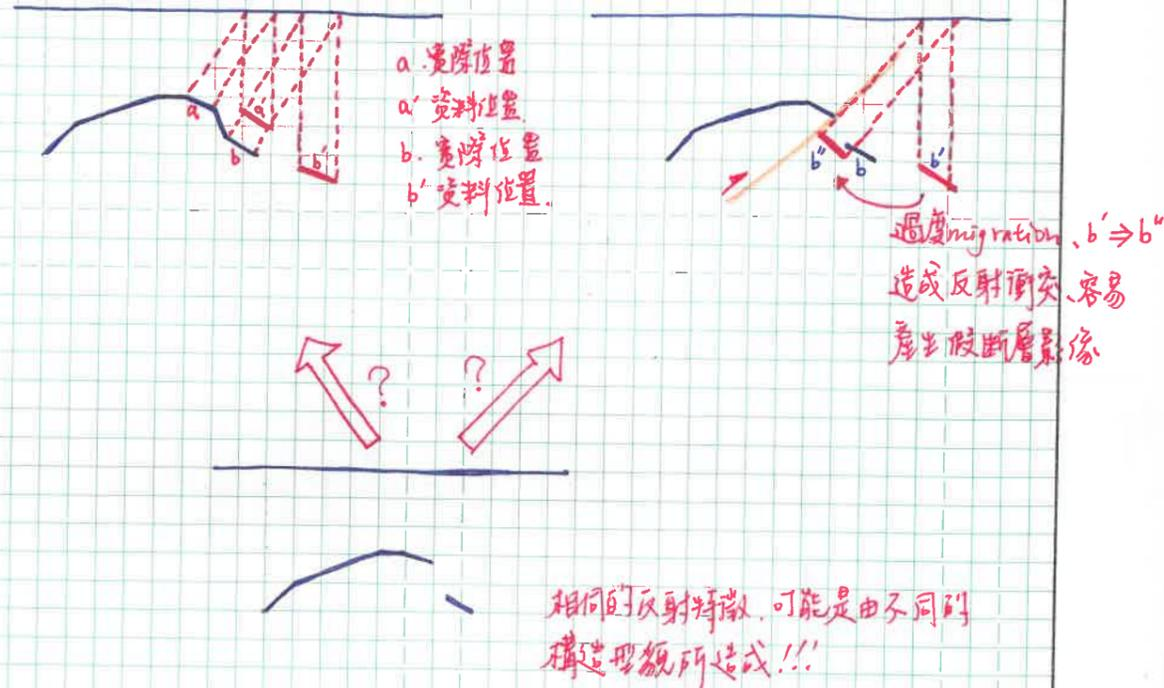
天氣：陰

日期：2018年10月14日 星期：日

• 要如何思考 Faulting vs Folding 問題

Rule of Model Based Processing

- 斷層或是褶皺的斷層都可能具有相同的反射特徵.
  - 需建立構造模型以便震測資料處理使用 (ex. PSDM)
- 但是，錯誤的模型會導致錯誤的資料處理和解釋結果。  
錯誤的解釋結果會導致錯誤的封閉構造描繪結果。



專題名稱：

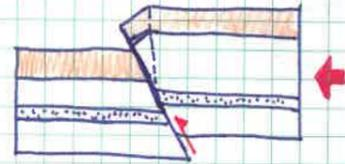
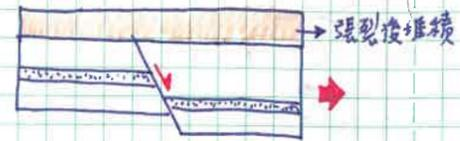
專題案號：

同 P65

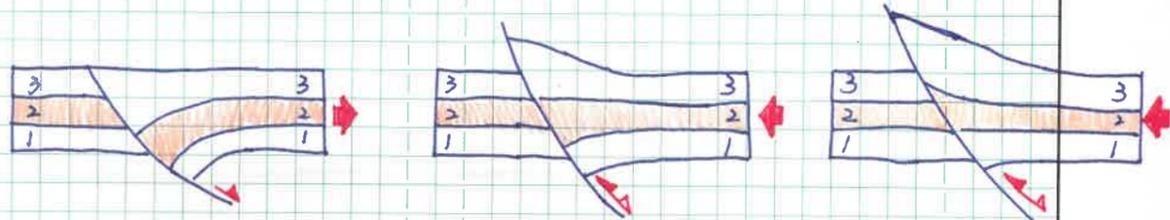
天氣：陰

日期：2018年10月14日 星期：日

9. Inversion and Reactivated Structures



若見到上昇盤厚度  
 大於下降盤  
 則指示此 Reverse Fault (正轉逆)



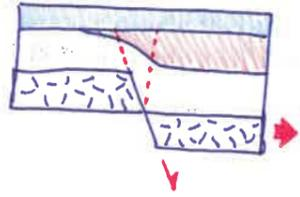
Criteria for Identifying Inversion Structures

→ Anomalous separation of units on fault.

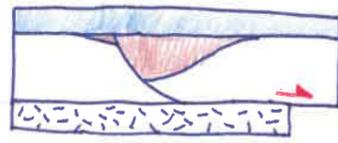
A null point separate units with normal and reverse separations.

→ Thicker extensional growth units on the upthrown block.

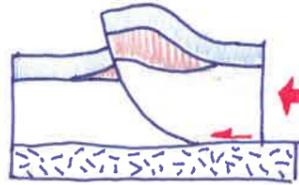
• Mechanisms of Inversion



Fault-Propagation Folding



Normal



Reverse.

Fault-Bend Folding

專題名稱：

專題案號：

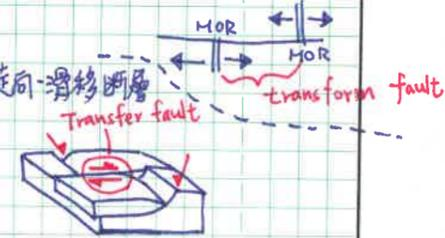
同 P65

天氣：陰

日期：2018年10月14日 星期：日

10. Strike-Slip Structures.

- Strike-Slip Faults and Structures 走向-滑移斷層及構造
  - Strike-slip fault: 為 general term. 可分為右移或左移走向滑移。
  - Wrench Faults 橫移斷層: 大尺度、極深、垂直、區域性地殼尺度的等同於 Transcurrent Faults.
  - Transform Faults 轉形斷層: Plate-bounding strike-slip fault that cut through the lithosphere 板塊邊界, 切穿岩石圈.
  - Transfer Faults 轉換斷層: 連結不同滑動斷塊間的走向-滑移斷層 strike-slip fault
  - Tear Faults 淺層橫移斷層, 埃斷層

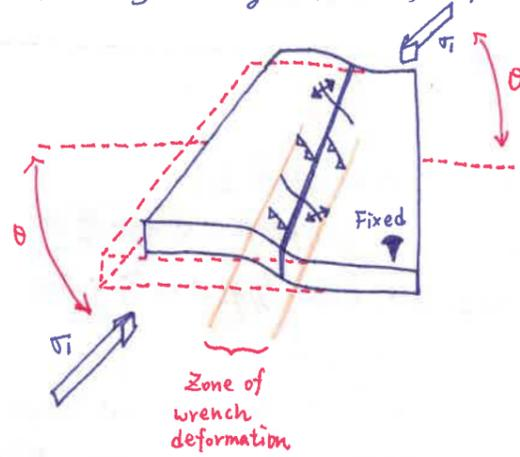


• Strike-Slip Structures. 走向滑移構造.

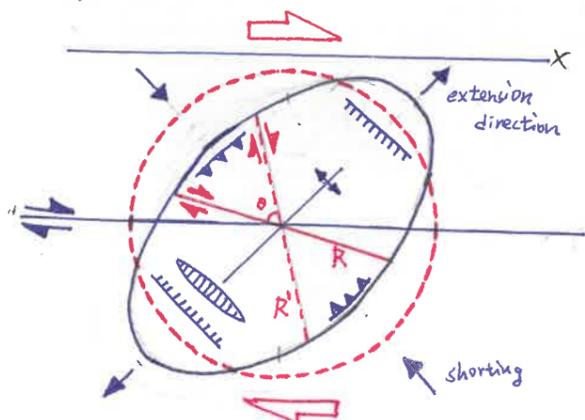
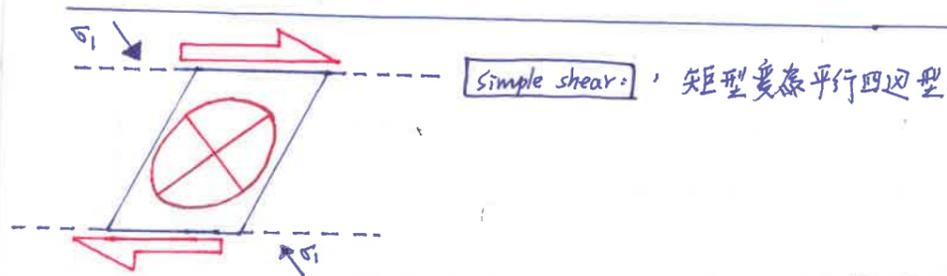
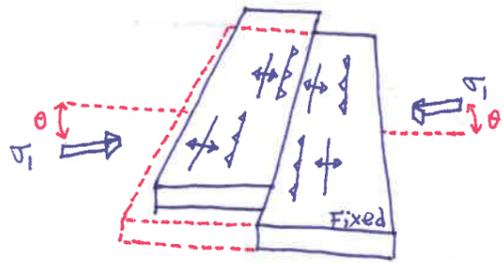
- Distributed v.s. Decoupled shear
- Distributed Shear - Secondary Structures
- Transpressive Structures - Positive Flower Structures
- Restraining Bends
- Transtensional Structures - Negative Flower Structures
- Releasing bends - Pull-Apart Basins

• Distributed v.s Decoupled Shear

\* High Drag 斷層不易移動 → Distributed Shear



\* Low Drag 斷層易移動 → Decoupled



应变椭圆 Strain Ellipse:

1. 褶皺和逆斷層與縮短方向 (shorting direction) 垂直.
2. 岩脈、正斷層與 extension 方向垂直
3. R 和 R' 與縮短方向成的交角皆為銳角.

- Vein
- Normal fault
- Thrust or Reverse fault
- Fold

$\theta \approx 60^\circ \sim 70^\circ$   
 synthetic strike-slip fault:  
 Antithetic strike-slip fault:

專題名稱:

專題案號:

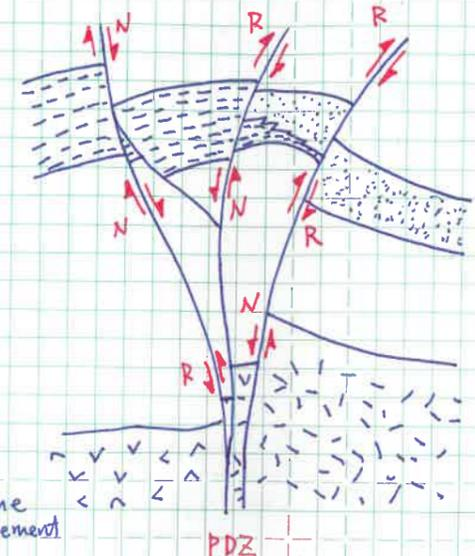
同 P65

天氣: 陰

日期: 2018年10月16日 星期: 日

• Transpressive Structures = ~~Positive~~ Positive Flower Structure  
 橫移壓縮 正花狀構造

若正花狀構造真的能在震測資料上, 應該正確的進行 3D 震測解釋.



N: Normal  
 R: Reverse

主要特徵:

- Basement involved
- Principle displacement zone (PDZ), sub-vertical at depth
- 垂直的斷層, 由線性或曲線狀的 PDZ 組成 strike-slip faults.
- Upward diverging & Rejoining splays

最常見的特徵就是雁形排列的斷層或褶皺 (但這些構造斜交)

斜接並置的岩石 juxtaposed rocks

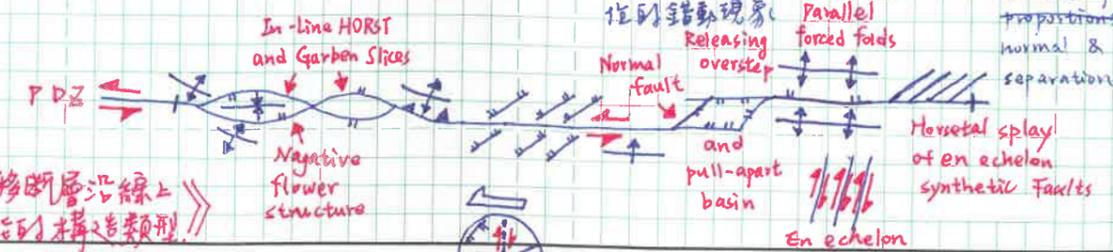
同一剖面上斷層距 separation

Successive Profiles

- Contrasting basement type 不同基底類型並列
- Abrupt variations in thickness & facies in a single stratigraphic unit. 厚度或沉積相的突變.

- Normal & Reverse - separation faults in same profile 同一剖面上同存正、逆斷層
- Variable magnitude & sense of separation for different horizon offset by the same fault. 同一斷層上 [有] 不同類型到錯動特徵, 或不同層位的錯動現象

- Inconsistent dip direction on a single fault. 同一斷層上, 有不同的傾向.
- Variable magnitude & sense of separation for a given horizon on a single fault.
- Variable proportion of normal & reverse separation faults.



左移斷層沿線上可能的構造類型

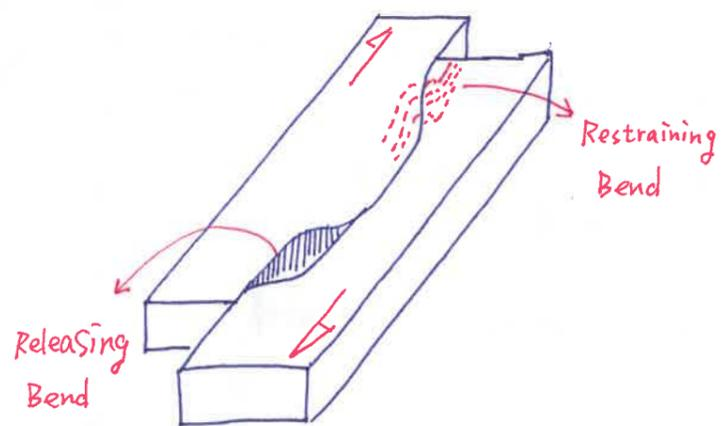
- vertical fault profile
- reverse fault



主管簽章:

• Restraining Restraining and Releasing Bends

p10



• Divergent Structure (Transitional structure): ~~Not~~ Negative Flower Structure

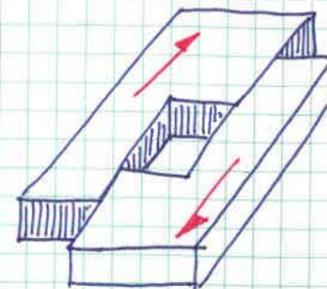
專題名稱:

專題案號: 同P65

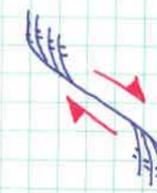
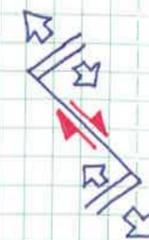
天氣: 陰

日期: 2018年10月14日 星期: 日

• Releasing Bends: Pull Apart Basin.



	Transform fault 轉形斷層	Transcurrent fault 橫移斷層
斷層兩端幾何型態	兩端點突然與其他地質構造相連。	端點會消失而轉變為區域性應變帶, 或分散為一系列小斷層
斷層沿線滑動數量變化方式	斷層沿線滑動數量可能比斷層長度長、短或相同。	由一點開始擴展, 斷層長度隨位移增加而變長。斷層位移量一定較斷層長度小。
斷層幾何型態隨時間演變方式	斷層上各位置的滑動量可以是相同的。	斷層的位移量在斷層線的中央最大, 向兩端逐漸變小。



15:56 end